SANDIA REPORT

SAND2010-8840
Unlimited Release
Printed January 2011

Modeling and Experimental Results for Condensing Supercritical CO2 Power Cycles

S. A. Wright, R. F. Radel, T. M. Conboy, and G. E. Rochau

Prepared by
Sandia National Laboratories
Albuquerque, New Mexico 87185 and Livermore, California 94550

Sandia National Laboratories is a multi-program laboratory managed and operated by Sandia Corporation, a wholly owned subsidiary of Lockheed Martin Corporation, for the U.S. Department of Energy's National Nuclear Security Administration under contract DE-AC04-94AL85000.

Issued by Sandia National Laboratories, operated for the United States Department of Energy by Sandia Corporation.

Available to DOE and DOE contractors from
U.S. Department of Energy
Office of Scientific and Technical Information
P.O. Box 62
Oak Ridge, TN 37831

Telephone: (865) 576-8401
Facsimile: (865) 576-5728
E-Mail: reports@adonis.osti.gov
Online ordering: http://www.osti.gov/bridge

Available to the public from
U.S. Department of Commerce
National Technical Information Service
5285 Port Royal Rd.
Springfield, VA 22161

Telephone: (800) 553-6847
Facsimile: (703) 605-6900
E-Mail: orders@ntis.fedworld.gov
Online order: http://www.ntis.gov/help/ordermethods.asp?loc=7-4-0#online

SAND 2010-8840
Unlimited Release
Printed January 2011

Modeling and Experimental Results for Condensing Supercritical CO_2 Power Cycles

S. A. Wright, R. F. Radel, T. M. Conboy, and G. E. Rochau
Advanced Nuclear Concepts Department
Sandia National Laboratories
P. O. Box 5800
Albuquerque, NM 87185-1136

Abstract

This Sandia supported research project evaluated the potential improvement that "condensing" supercritical carbon dioxide (S-CO_2) power cycles can have on the efficiency of Light Water Reactors (LWR). The analytical portion of research project identified that a S-CO_2 "condensing" re-compression power cycle with multiple stages of reheat can increase LWR power conversion efficiency from 33-34% to 37-39%. The experimental portion of the project used Sandia's S-CO_2 research loop to show that the as designed radial compressor could "pump" liquid CO_2 and that the gas-cooler's could "condense" CO_2 even though both of these S-CO_2 components were designed to operate on vapor phase S-CO_2 near the critical point. There is potentially very high value to this research as it opens the possibility of increasing LWR power cycle efficiency, above the 33-34% range, while lowering the capital cost of the power plant because of the small size of the S-CO_2 power system. In addition it provides a way to incrementally build advanced LWRs that are optimally designed to couple to S-CO_2 power conversion systems to increase the power cycle efficiency to near 40%.

Executive Summary

This "late start" LDRD project evaluated the potential improvement that "condensing" supercritical carbon dioxide (S-CO_2) power cycles can have on the power conversion efficiency of Light Water Reactors (LWR). The research was performed over a period of about 3-4 months and consisted of both analysis and experiments. The analytical portion of research project identified that a S-CO_2 "condensing" re-compression power cycle with multiple stages of reheat can increase LWR efficiency to ~37-39%, according to computational models. Typical LWRs using steam turbines operate closer to 33-35%. The experimental portion of this project used Sandia's S-CO_2 research loop to show that the as-designed radial compressor could efficiently "pump" liquid CO_2 and that the gas cooler could "condense" CO_2, even though both of these components were designed to operate using single phase CO_2 near the critical point.

There is potentially very high value to this research, as it opens the possibility of increasing LWR power cycle efficiency above the 33-35% range, while lowering the capital cost of the power plant due to the small size of the S-CO_2 power system (Wright et al, 2010). In addition this provides a way to incrementally build advanced LWRs that are optimally designed to couple to S-CO_2 power conversion systems, to further increase the power cycle efficiency beyond 40%.

The research project consisted of two portions, an analysis portion and an experimental portion. The first portion performed a series of power cycle analysis to assess the potential of S-CO_2 power systems to increase the efficiency in LWRs. The power cycle that appears most suitable for LWRs is the "condensing" re-compression cycle with multiple stages of reheat. The second effort performed a series of experimental tests using the Sandia S-CO_2 compression test-loop to validate the ability of these power systems to actually operate in the condensing mode.

For the experimental effort, three types of tests were performed. First a series of tests were performed to show that the radial compressor could effectively compress liquid CO_2, despite being designed to operate near the critical point. The second series of tests operated the S-CO_2 test loop to show that the radial compressor and other components of the S-CO2 test loop could be operated with a single-phase liquid, a supercritical vapor, or with two-phase saturated vapor/liquid mixtures. The third effort required modification of the S-CO_2 research loop by adding a small heater (50 kW) to increase the temperature of the CO_2 after compression. With the addition of the heater it was then possible (in one experiment) to provide a saturated vapor or a two-phase mixture to the tube and shell heat exchanger that condensed the fluid in the gas cooler, and then "pump" the liquid phase CO2 with the radial compressor. This last series of experiments demonstrated that condensation occurred in the gas cooler and that the resulting liquid could be pumped by the S-CO_2 compressor.

The results of the research effort have therefore demonstrated that the small-scale proof-of-concept design of the Sandia re-compression Brayton cycle is capable of both condensing the CO_2 in the gas cooler and pumping liquid in the S-CO_2 main compressor. Overall the analysis

and the experimental test results performed for this research project effectively demonstrate that the proposed power cycle for the LWR S-CO_2 power plant can operate in the "condensation" mode. When operated with pure CO_2 the "condensing" mode requires heat rejection with an exit temperature less than 31 C (88 F); however, this can be relaxed if current research on CO_2 gas mixtures demonstrate the ability to increase the effective critical temperature. When this "condensing" power mode of operation is used with a re-compression power cycle having multiple- stages of reheat, it can increase LWR power plant efficiency to near 40% and beyond.

NOMENCLATURE

ASME	American Society of Mechanical Engineers
BNI	Barber-Nichols Incorporated
BWR	Boiling Water Reactor
CFD	Computational Fluid Dynamics
CO_2	Carbon Dioxide
DOE	Department of Energy
FEA	Finite Element Analysis
GenIV	Generation IV International Forum
IGBT	Insulated Gate Bipolar Transistor
LDRD	Laboratory Directed Research & Development
MAWP	Maximum Allowable Working Pressure
MCFV	Main-Compressor-Flow-Valve
NASA	National Aeronautics and Space Administration
NIST	National Institute of Standards and Technology
NRC	Nuclear Regulatory Commission
OD	Outside Diameter
PID	Proportional–Integral–Derivative
PWR	Pressurized Water Reactor
Refprop	NIST Reference Fluid Thermodynamic and Transport Properties Database
RPCSIM	Reactor Power and Control SIMulation code
RTD	Resistance Temperature Detectors
S-CO_2	Supercritical Carbon Dioxide
SCR	Silicon Controlled Rectifier
SNL	Sandia National Laboratories
TAC	Turbo-Alternator-Compressor
TRACE	TRAC/RELAP Advanced Computational Engine
T-D	Temperature-Density
T-S	Temperature-Entropy

Table of Contents

Table of Figures

Table of Tables

1 Introduction

1.1 *Background*

Advanced power conversion systems that optimally couple to the thermal output characteristics of next generation advanced reactors have the potential to provide higher efficiency nuclear electricity at lower costs. Improvements in plant efficiency can increase plant electrical output directly and have the same impact as direct reductions in plant construction and operating costs. There can be additional cost savings, if the power conversion system capital costs can also be reduced in comparison to current systems. Therefore, there is significant motivation to investigate power conversion system approaches that can maximize the power output of advanced reactor systems.

Supercritical Brayton cycles and other advanced supercritical cycles are one of the most promising approaches to achieving higher efficiency and more cost effective power conversion. These cycles have the potential to achieve higher efficiencies across the range of advanced reactor outlet temperatures, because the high power densities and liquid-like working-fluid densities everywhere in the system allow for the use of extremely compact power conversion machinery. Large-scale supercritical CO_2 systems are estimated to be about 1/10th the size of a comparable steam Rankine cycle, and therefore also have the potential to reduce power conversion system capital costs, resulting in additional savings.

The supercritical CO_2 systems also have strategic value because of their small size, transportability, and ability to couple to any heat source including solar, geo-thermal, fossil, and nuclear systems. The Department of Energy (DOE), Department of Defense (DoD) and a number of industrial companies have active programs exploring supercritical CO_2 power systems for all the above mentioned heat sources.

The DOE Generation IV program has been exploring the use of supercritical CO_2 Brayton cycles for use in LMRs because the operating temperature is ideally suited to the S-CO_2 Brayton power system. Because of the lower operating temperature of LWR reactors (~325°C), LWRs have generally not been considered as candidates for S-CO_2 power systems. However the research in this project shows that S-CO_2 power systems can also be applied to LWRs when the appropriate power cycle is used, allowing LWR reactors to reap the benefits of small size, reduced capital costs, and improved cycle efficiency as well. The improvement in efficiency at the lower LWR temperatures requires a slightly different thermodynamic power cycle than used in LMRs. The proposed LWR power cycle is a condensing re-compression power cycle with multiple (two) stages of reheat. This power cycle was originally described by Angelino (1969) and more recently summarized by Dostal (2004).

1.2 *"Condensing Power Cycle"*

The key feature that makes proposed cycle work for S-CO_2 power systems is the "condensation" that occurs in the waste heat rejection unit. The slightly lower temperature (<31C / 88F) required for condensation lowers the compressor inlet pressure, which increases the fluid density, increases the compression ratio and allows for multiple stages of turbine reheating. In steam systems the condenser is a very large because it operates at a vacuum (5 kPa or ~ 1psia). It also

uses gravity to separate the liquid from the vapor to feed the water pump with a large density difference between the liquid and the vapor (1000:1). In an S-CO_2 power system, the waste heat rejection occurs at high pressure (> 6 MPa ~ 900 psia) that is near the critical point; therefore the fluid density is high even for the vapor. (0.75 kg/l liquid and 0.21 kg/l for the vapor). The liquid/vapor density ratio is only a factor of 3:1, not 1000:1 as for steam systems. Because of this small density ratio, the radial compressor can "pump" liquid CO_2. It can also "pump" the supercritical vapor, or the two-phase mixture. The experimental research performed for this LDRD project verify that:

1) the tube and shell gas cooler can effectively condense the CO_2 even though it was not designed as a condenser, and
2) the radial compressor effectively compresses ("pumps") the liquid CO_2 even though it was designed to operate at the critical point of CO_2 (no degradation in compression efficiency is observed),
3) the compressor can also pump the vapor phase as well as the two-phase vapor-liquid mixture.

The condensing waste heat rejection means that the S-CO_2 power system operates essentially as a recuperated Rankine power cycle, even though it was designed to be a re-compression Brayton cycle. An important benefit of this research, is that it shows that the S-CO_2 power system can take advantage of lower heat rejection temperatures (when they are available such as in winter or in colder climates) by simply allowing the gas-cooler to condense the CO_2. This will increase the net power cycle efficiency, increase the generated power, and improve the economics without requiring hardware modifications to the power plant. Another benefit is that the lower pressures that accompany the lower heat rejection temperature make it easier to use multiple stages of reheat to further improve the cycle efficiency. Thus, the combination of condensing S-CO_2 re-compression power cycles, and multiple stages of reheat, are able to allow S-CO_2 power systems to be applied to LWRs as well.

This research project investigated supercritical CO_2 power systems that use multiple reheat stages and a condensing heat rejection unit (similar to the Rankine cycle) to increase the cycle efficiency of LWRs, . A typical LWR operates at peak mixed mean exit temperatures near 325°C. At turbine inlet temperatures of 315°C and a compressor outlet pressure of 20.6 MPa, the supercritical CO_2 condensing power system has a cycle efficiency of approximately 37-39% depending on assumed environmental operating temperatures and pressures (295-300K (71-80 F). The efficiency gains occur because the reheating cycle and the condensing heat rejection allows the system to operate more closely to the ideal Carnot cycle. The system remains small because the fluid densities are large compared to the standard steam Rankine cycle system which must operate at a vacuum in the condenser. It also appears likely that a pressurized water reactor when connected to a "condensing" S-CO_2 power system could approach efficiencies near 40% by increasing the secondary CO_2 loop pressure to 25 MPa while maintaining the same peak turbine inlet temperature of 315°C.

1.3 *Research Project*

The research project presented here consists of two portions, an analysis portion and an experimental portion. The first portion performed a series of power cycle analyses to assess the

potential of S-CO_2 power systems to increase the efficiency by using a "condensing" re-compression power cycle. This power cycle was first described by Angelino (1969) and later reviewed by Dostal (2004). The second effort consisted of performing a series of experimental tests using the Sandia S-CO_2 compression test-loop to validate the ability of these power systems to actually operate in the condensing mode.

Three types of experiments were performed. First, a series of tests were performed to show that the radial compressor could efficiently compress liquid CO_2, even though it was designed to operate near the critical point. The second series of tests involved operating the S-CO_2 test loop at constant pressure while adjusting the fill inventory of the loop to move the compressor inlet conditions from a liquid, through the two-phase region, and then to the vapor side of the saturation curve. The last experiment required modifying the loop by adding a small heater (50 kW) that increased the temperature of the CO_2 after compression. The heated CO_2 was then expanded in a motor driven nozzle to either to a saturated vapor or to a two phase mixture. The saturated vapor or the two-phase fluid was then condensed in the tube and shell spiral heat exchanger. The results of these tests showed that the existing gas cooler was able to condense both the single phase vapor and two-phase CO_2 into a liquid. The gas cooler design is described in Wright (Wright et al, 2010). It was not designed to condense the fluid, and it had no provisions to separate the liquid from the gas phase. Nevertheless, it was fully capable of condensing the fluid under the conditions at which it was tested. Other S-CO_2 testing with printed circuit heat exchangers are also showing similar results, though these tests are still in progress. This flexibility in the thermal operating range for these heat exchangers is believed to be due to the small density difference between liquid CO_2 and vapor CO_2, which is only a factor of 3:1, in comparison to water which has a density ratio of 1000:1.

The combination of these experiments confirms the validity of the analytical result, and provides strong evidence that S-CO_2 power systems designed to operate (reject heat) near the critical point can, when environmental conditions permit, reject heat at lower temperatures and thereby increase the power cycle efficiency. This makes it extremely likely that the "condensing" re-compression cycle with reheat proposed here can be used to significantly increase the power generation efficiency, and extend the operating temperature range sufficiently that they can be used for LWR systems.

A separate experimental program is examining the possibility of removing the restriction of low heat rejection temperatures by exploring the use of using mixtures of CO_2 and other fluids to increase (or if desired lower) the critical point of the mixture. If this research proves successful, then the "condensing" power cycle can be extended to higher heat rejection temperatures, thereby providing efficiency benefits at temperatures well above 31 C (88 F).

The following report begins by describing the "condensing" S-CO_2 power cycle and shows how it is used to increase the cycle efficiency. The next section describes the experimental test results. It begins with a short description of the test hardware that was used to validate S-CO_2 operations in the liquid, vapor, and two-phase regimes. The last section describes the results of the three experiments that were performed with liquid CO_2, two-phase CO_2 and with condensing CO_2.

2 Condensing S- CO_2 Power Systems and Their Potential

The use of supercritical CO_2 power cycles for advanced nuclear reactors was described by Dostal (Dostal, 2004) from the Massachusetts Institute of Technology (MIT). The power cycle identified as having the highest efficiency is the re-compression cycle, which also has other advantages in that it avoids recuperator pinch points and uses fewer hardware components than other cycles. Since these recent analytical reports from MIT, Sandia National Laboratories (Sandia) and the Department of Energy (DOE) have supported a hardware S- CO_2 research effort by funding proof of concept S- CO_2 research loops. These projects are hardware focused and have resulted in the development of a supercritical compression loop and a Brayton cycle loop that can be configured as a re-compression cycle or a simple Brayton cycle. The compression loop is described in the next section, and the dual-turbomachine re-compression Brayton loop in Wright (Wright et al, 2008).

The research compression loop is located at Sandia, while the re-compression Brayton loop is located at Sandia's contractor site at Barber Nichols Inc in Arvada, Colorado. The compression loop was built to investigate the issues of compression and control near the critical point, but also has been instrumental in developing the key technologies (bearings, seals, windage friction modeling, motor/generator control) required to successfully operate the turbomachinery. The dual-turbomachine re-compression Brayton cycle is in its final phases of development. It is currently being used to investigate the ability of the S-CO_2 cycle to generate electricity, simultaneously validating our turbomachinery models as well as other S-CO_2 component models, including heaters and printed circuit heat exchangers (Heatric 2010). Dynamic systems models are also being developed and validated.

2.1 *The Condensing Power Cycle for Moderate to High Turbine Inlet Temperatures > 450 C.*

A schematics of a typical re-compression Brayton cycle connected directly to the reactor coolant through a primary heat exchanger is illustrated in Figure 2-1 while the temperature and pressure state-points are shown in Figure 2-2. In the supercritical power cycle the turbomachinery is small because of the high density of the fluid (see figure) and because only a few stages (1-3) of turbine or compressor stages are needed (Barber Nichols Inc. 2006, and Pratt and Whitney Rocketdyne 2006). In addition the efficiency is high because the compressor work is low and because the re-compression cycle allows the recuperators to transfer 3-4 times more heat than is provided by the primary heat exchanger. The highly recuperated loop means that the heat is transferred to the CO_2 fluid over a limited temperature range (~150 K) which increases the cycle efficiency. Typical state points for this power cycle when connect to a LMR operating at a mixed mean exit temperature near 823 K (550 C) are illustrated in Figure 2-3 for a 97.7 MWe power plant and a power cycle efficiency of 45.5%. The cycle analysis assumes 5% pressure drop in the loop and uses 85%,87%, and 90% for the main-compressor, re-compressor, and turbine.

The temperature-entropy (T-S) diagram for the Brayton cycle is shown by the red curve in Figure 2-3. The "condensing" power cycles is the same cycle except that the gas cooler now

condenses the CO_2 to provide the compressor inlet with a saturated liquid. The cycle diagram for both cycles is presented in Figure 2-3 because it illustrates the efficiency gains that can be obtained by operating this cycle in a condensing mode, as shown by the blue lines. The larger enclosed area means greater power generation and greater efficiency, which is the reason for the interest in this condensing cycle. In this analysis the "condensing" cycle increases the efficiency to 48.3% for the same peak turbine inlet temperature. The condensing re-compression cycle was originally described in a series of reports by Angelino, (Angelino, 1967, 1968, and 1969), and it provided the foundation for the MIT research by Dostal (Dostal, 2004).

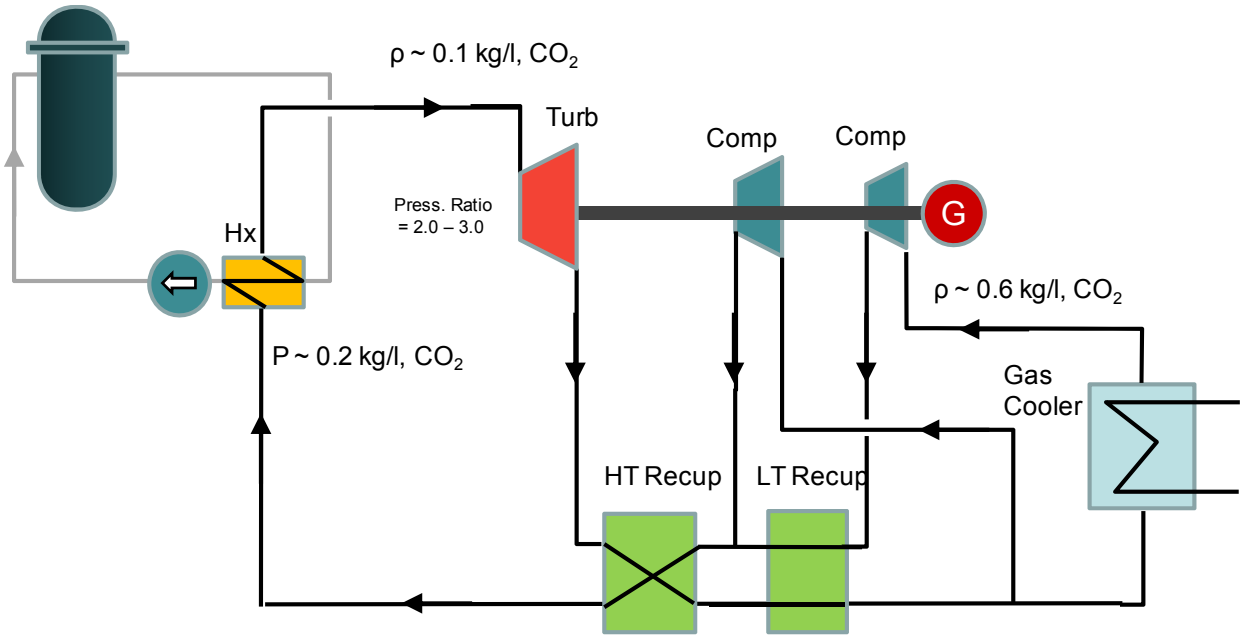

Figure 2-1: Schematic of supercritical CO_2 re-compression Brayton cycle. The cycle is shown connect to a reactor through a heat exchanger.

In the condensing power cycle, the waste heat cooler condenses the CO_2 to a saturated liquid, at the compressor inlet, rather than a gas as in the Brayton cycle. This means that the CO_2 waste heat rejection temperature and pressure both must be less than the critical point (304.1 K and 7377 kPa). As was mentioned previously, the T-S diagram of the condensing power cycle and the Brayton cycle shown in Figure 2-3 reveals a larger enclosed area for the condensing cycle because of the condensation process and because of the lower pressure in the low pressure leg of the power cycle. The T-S curves shown in Figure 2-3 were made for the peak temperature and pressure conditions that are appropriate for liquid metal reactors as shown in Figure 2-2. For illustration purposes the condensing cycle used a heat rejection temperature of 292.5 K (66.8°F) which corresponds to a saturation vapor pressure of 5642 kPa.

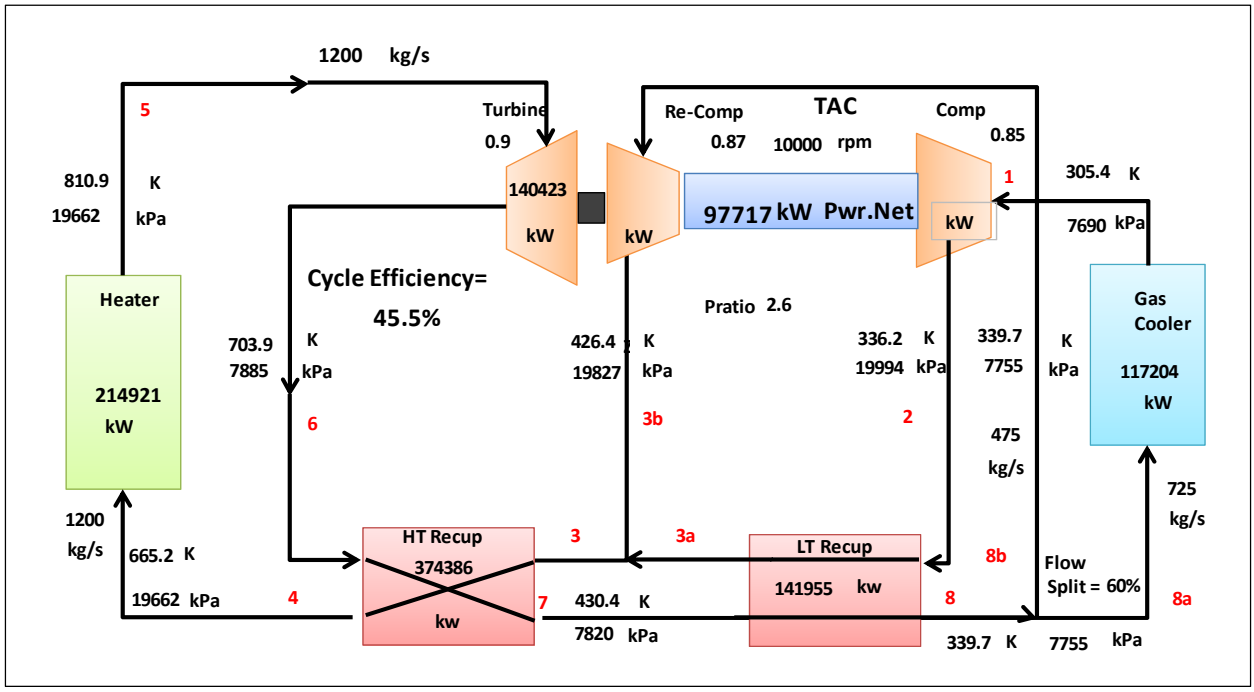

Figure 2-2: Schematic flow diagram of a re-compression S- CO_2 Brayton cycle. The temperature and pressure, and flow rate for typical S- CO_2 operating conditions are shown here for a 104 MWe power system. The cycle analysis assumes a 5% pressure drop throughout the system (approximately 1% per component).

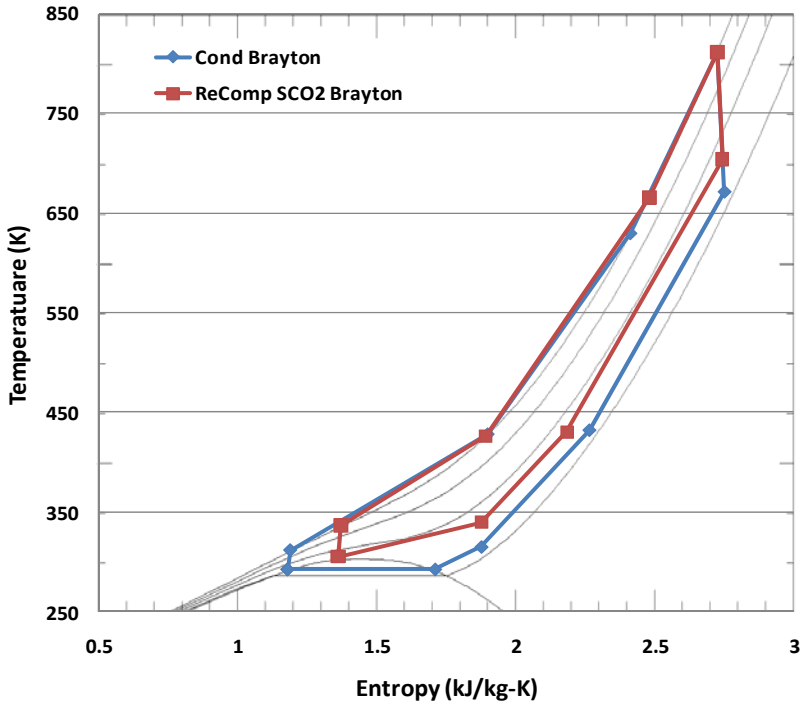

Figure 2-3: T-S diagram illustrating the re-compression S- CO_2 Brayton cycle (red) and condensing re-compression power cycle (blue). Both systems have a turbine inlet T of 810 K and a peak pressure of 20 MPa. The lines of constant pressure are shown at 5, 10, 15 and 20 MPa.

For the "condensing" power cycle, the power conversion efficiency will increase as the heat rejection temperature is lowered. Figure 2-4 illustrates the cycle efficiency as a function of heat rejection temperature for the condensing power cycle and for a few selected points on the re-compression Brayton cycle. Estimates of power cycle efficiency were made based on models developed in Microsoft Excel, and evaluated using its solver feature. As can be seen, there is a marked improvement when using the condensation cycle at lower heat rejection temperatures. Lowering the compressor inlet temperature from 305K to 300K (80.3°F) increases the cycle efficiency by over 1.5%, and lowering it to 295 K (71.3°F) increases the cycle efficiency by 2.7%. For large power systems these are large increases in efficiency and they can have a strong impact on the economics of the power plant.

Unfortunately, the condensation cycle requires a lower compressor inlet temperature that may not be achievable at all power plant locations. In northern latitudes or during winter, many locations within the U.S. will; however, be capable of operating at these lower compressor inlet temperatures. Nevertheless, it is highly desirable that a real power plant be able to take advantage of better heat rejection capability when it is available due either to location or time of year. Steam Rankine cycles do take advantage of colder heat sink temperatures when available. Originally it was thought that the re-compression Brayton cycle would not be able to take advantage of these cooler inlet operating conditions, because the S-CO_2 recompression Brayton cycle was designed to operate at a fixed compressor inlet temperature and pressure that is near the critical point 304.3 K (88°F). However, the experimental testing in this project reveals that the re-compression Brayton cycle components (compressor and gas cooler) can indeed operate in the condensing mode even though they were not specifically designed for these conditions. It is believed that the flexibility of the S-CO_2 system is possible because the density difference between liquid and vapor CO_2 is only a factor of two or three, in contrast to water, where the density difference in the condenser is a factor of 1000.

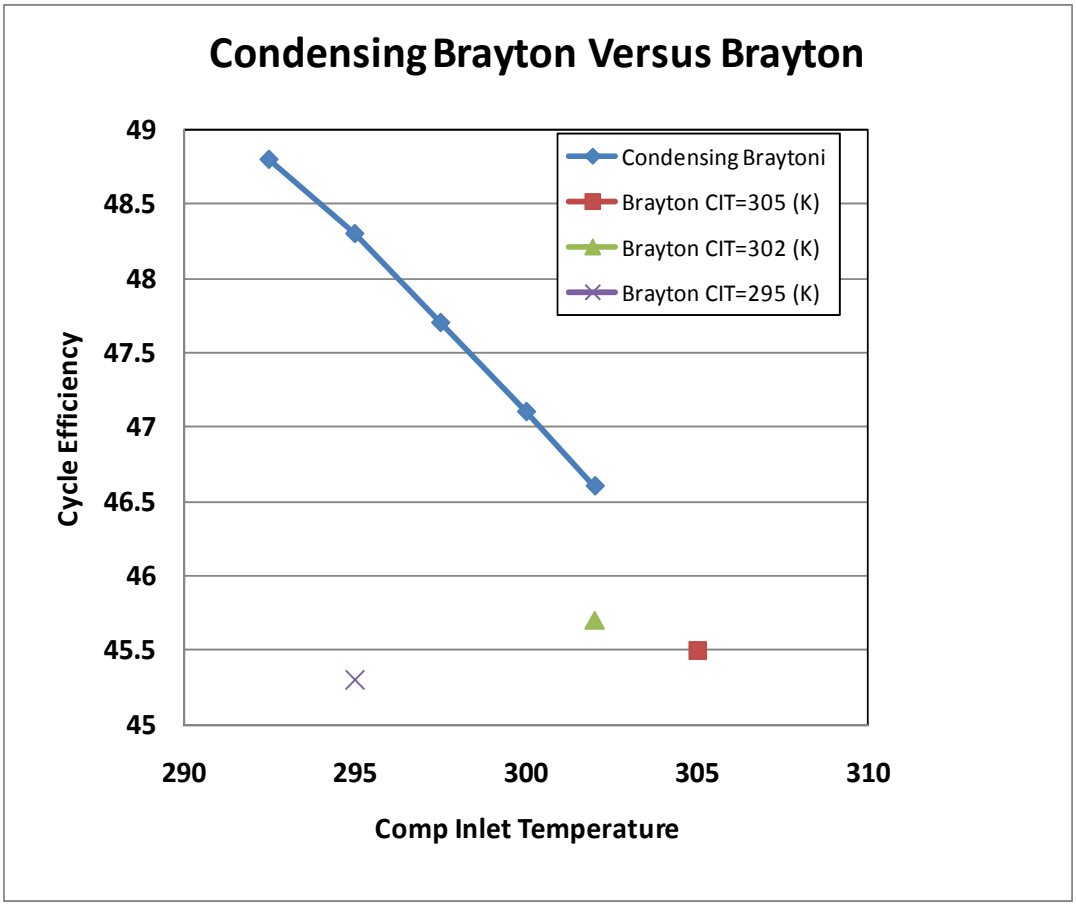

Figure 2-4: An illustration of how lowering the compressor inlet temperature (condensation temperature) increases the efficiency of the power condensation cycle. The blue curve shows the cycle efficiency of the condensing re-compression power cycle as a function of condensation temperature, the points show the efficiency of a corresponding Brayton cycle at the same peak compressor outlet pressure of 20 MPa but 295, 302 and 305 K. As can be seen, there is a marked improvement when using the condensation cycle at lower heat rejection temperatures.

Furthermore it is likely that the temperature restrictions on condensation may even be relaxed. Other supercritical power cycle research at Sandia indicates that it may be possible to "tune" the critical temperature and pressure (either up or down by up to 15-20 K) of the CO_2 fluid by adding in mixtures of other gases to CO_2. These tests are still in progress and the results are not yet available. However the Refprop (Lemmon et al, 2007) properties predict these effects. A technical advance document for patent applications is in process for "tuning" the critical point based on gas mixtures with CO_2. (Wright SD11594, 2010, Sandia, SNL sub proposal to ORNL CEEB-180, February, 2009). If this "tunable" gas mixture approach is successful, it will also likely be possible to operate these systems in a condensation mode as well. This will greatly extend the capability of supercritical power systems and allow for maximum efficiency under a wide range of conditions including latitude, time of year, or perhaps even time of day.

The preceding discussion shows that the condensing re-compression power cycle can increase the cycle efficiency for power systems operating at a turbine inlet temperature of 450 – 750°C by about 2.5 to 3 percentage points for a 10 K reduction compressor inlet temperature (about 71°F).

To achieve the efficiency gains, it also requires a greater pressure rise in the pump/compressor, and requires that the waste heat exchanger provide liquid CO_2 to the compressor/pump inlet. Experimentally verifying these capabilities was the goal of this research project. Another goal of this project was to determine which S- CO_2 power cycle might provide the most advantage for (LWRs). This topic is described in the next section.

2.2 *Supercritical CO_2 power systems for Light Water Reactors*

Supercritical CO_2 power systems have largely focused on the intermediate temperature range from 450°C – 750°C (723 K to 1023 K). S- CO_2 power systems are ideally suited for liquid metal cooled reactors (LMRs) and other reactors that operate at these temperatures. This section of the report identifies a supercritical CO_2 power cycle that may provide efficiency benefits for LWRs. The power cycle that was selected for LWRs is the condensing re-compression cycle with two stages of reheat which is schematically illustrated in Figure 2-5 and a table of the state-points is presented in Table 2-1. The T-S diagram for this cycle is illustrated in Figure 2-6 and is compared again to the re-compression Brayton cycle. The condensing cycle with reheat operates at a turbine inlet temperature of 588 K (315°C) and a pressure of up to 20 MPa. The reheating requires two additional heat exchangers that reheat the CO_2 after partial expansion in the turbines. The re-heaters operate at near 15 and 11 MPa, while the main heat exchanger operates at 20 MPa. The cycle efficiency is shown to be 38.7% at 315°C, which is a significant improvement over existing LWRs that operate at efficiencies near 33-35%. Higher LWR reactor outlet temperatures near 350°C (rather than 320°C) could further increase the cycle efficiency to 41%. The estimates of power cycle efficiency were made based on models developed in Microsoft Excel, and evaluated using its solver feature.

Table 2-1: State point values at entrance and exit of each component in the condensing power cycle with 2 stages of reheat. The compressor and turbine efficiencies were assumed to be 90% and 93% which is consistent with predicted efficiencies for multi-hundred Megawatt systems. For comparison the state points for a re-compression Brayton cycle are shown on the right side of the table.

	Condensing Cycle with 3 Stages of Reheat					Re-Compression Brayton	
Station	T (K)	s (kj/kg-K)	h(kJ/kg)	d (kg/m^3)	p (kPa)	T (K)	s (kJ/kg-K)
1	295.00	1.209	262.38	752.56	5982.17	305.0	1.341
2	316.08	1.215	282.81	830.79	20685	333.2	1.347
3	428.89	1.893	530.32	325.82	20513	420.7	1.873
4	512.04	2.148	649.01	230.37	20342	659.8	2.473
5a	588.15	2.326	745.77	186.90	20172	810.9	2.728
6a	559.66	2.329	720.18	151.80	15493	700.6	2.741
5b	588.15	2.389	754.76	142.28	15364		
6b	551.12	2.395	720.90	108.02	10814		
5c	588.15	2.473	764.08	142.28	10723		
6c	531.63	2.480	710.91	108.02	6134		
7	432.89	2.256	602.21	98.86	6083	424.7	2.172
8	319.08	1.877	461.55	62.98	6032	336.2	1.860
1 Sat. Vap	295	1.688	403.64	209.72	6032	305.0	1.341
1 Sat Liq	295	1.209	262.38	752.56	6032		

Incrementally increasing LWR outlet temperatures to 350°C and using supercritical CO_2 systems with reheat in condensing cycles seems more likely to provide near term reactor power generation and efficiency benefits, over the alternative LWR energy efficiency options. These

other options generally make use of supercritical water reactors (SCWR) that operate in the range from 500°C and have an efficiency of 44.8% (Buongiorno, 2003). Though coal fired power plants do operate with supercritical steam, it is very problematic for a LWR to operate at past the critical temperature (373 C) because of adverse density and heat transfer effects that occur in the reactor due to the nature of supercritical steam and also because of accelerated corrosion. To avoid some of these very issues, recent SCWR concepts are being proposed that limit the primary circuit to 380 C, at 25 MPa and have a power cycle efficiency of 37.5% (Vogta, 2010).

To realize the potential benefits of S-CO_2 systems, the LWR industry and DOE would need to demonstrate that a S-CO_2 power system can provide efficiency improvements over conventional steam systems. To achieve the incrementally higher temperatures it must also be shown that the reactor, fuel, and cladding can also operate at these higher conditions. An advanced LWR experimental testing program will ultimately have to be performed to validate the ability to safely increase the reactor temperature and pressure to higher pressurized mixed mean water outlet conditions near 350°C. If both the demonstration power system proves advantageous, and solutions are found to incrementally increase the reactor outlet conditions, then it might be possible to install a S-CO_2 power system on an LWR to demonstrate its economic advantage. An increase of 5 percentage points in power conversion cycle efficiency (from 33% to 38%) will result in a 15% increase of electricity output from the same thermal power input. This translates to a 15% increase in revenue for that power plant.

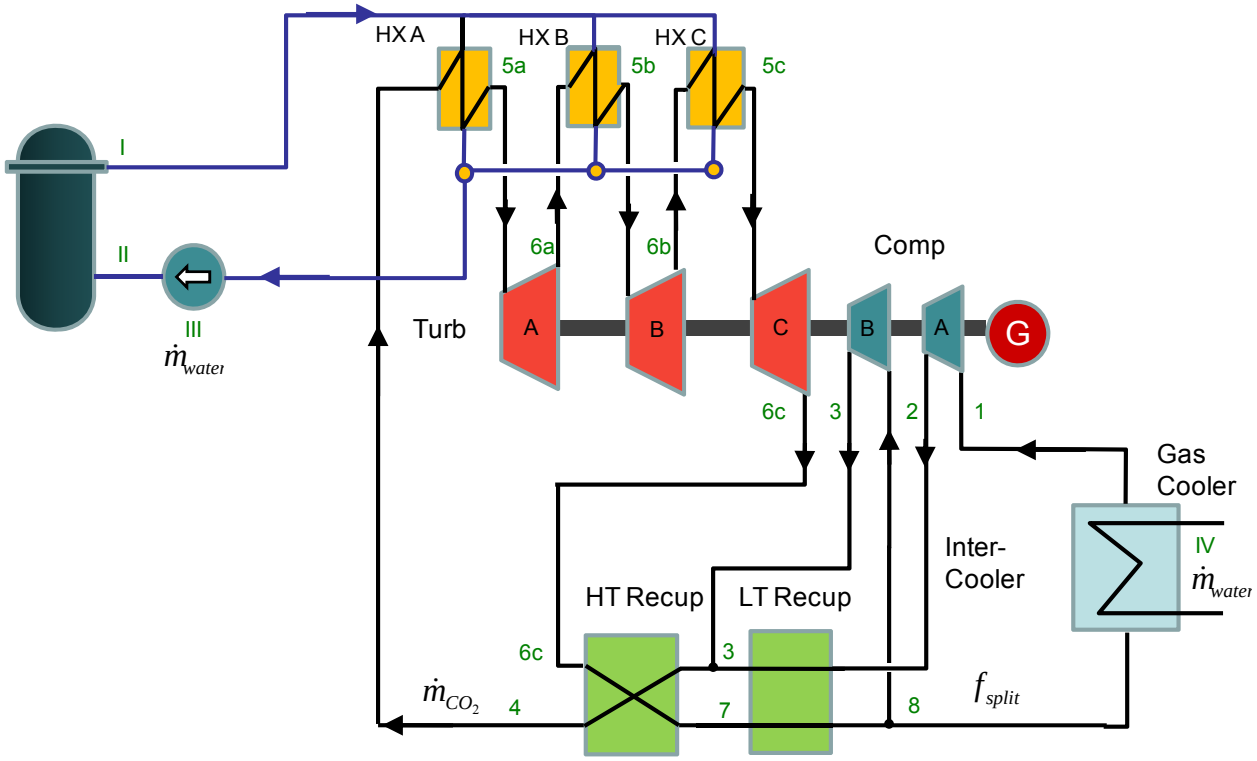

Figure 2-5: "Condensing" re-compression split-flow "condensing" power cycle with two stages of reheat.

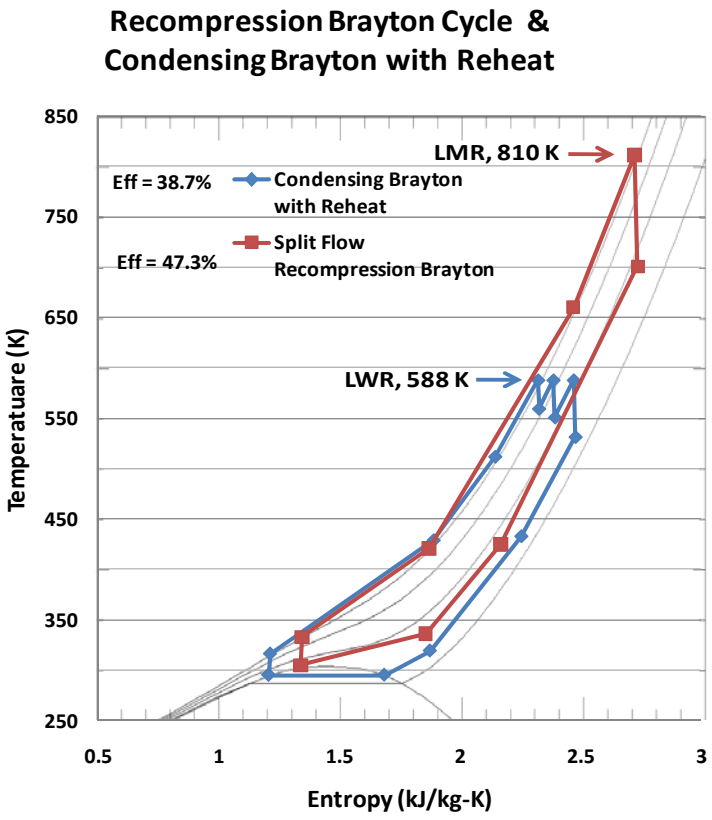

Figure 2-6: A comparison of a supercritical re-compression system operating at liquid metal reactor temperatures and a condensing Brayton with reheat operating at LWR temperatures.

3 S-CO_2 Compression Test Loop Hardware

The primary goal of this LDRD project is to use Sandia's available S-CO_2 hardware, with minor modifications, to demonstrate the viability of the condensation cycle. These experiments, which are described in the next section, provide the first hardware demonstration for condensing CO_2 power cycles. These experiments show that the turbomachinery, heat exchangers, and the entire loop are capable of operating in the condensing mode, even though the components were designed to operate in the single phase region near the critical point.

Initial experiments for this LDRD utilized a compression test loop designed and built by Sandia and its contractor Barber Nichols Inc. (Barber Nichols, 2008) to investigate the key technology issues associated with the standard S-CO_2 Brayton cycle. Details on the design and operation of this loop can be found in a previous LDRD report (SAND2010-0171). Figure 3-1 shows an engineering drawing of the SNL supercritical compression test-loop. The loop sits on a skid that is approximately 2m x 3m and contains a motor-driven radial compressor, its motor/alternator controller, a Coriolis flow meter, a pressure drop valve, a tube-and-shell gas-chiller, and miscellaneous compressors and ducting to control the rotor cavity pressure to reduce windage losses and to allow for fill and purge operations.

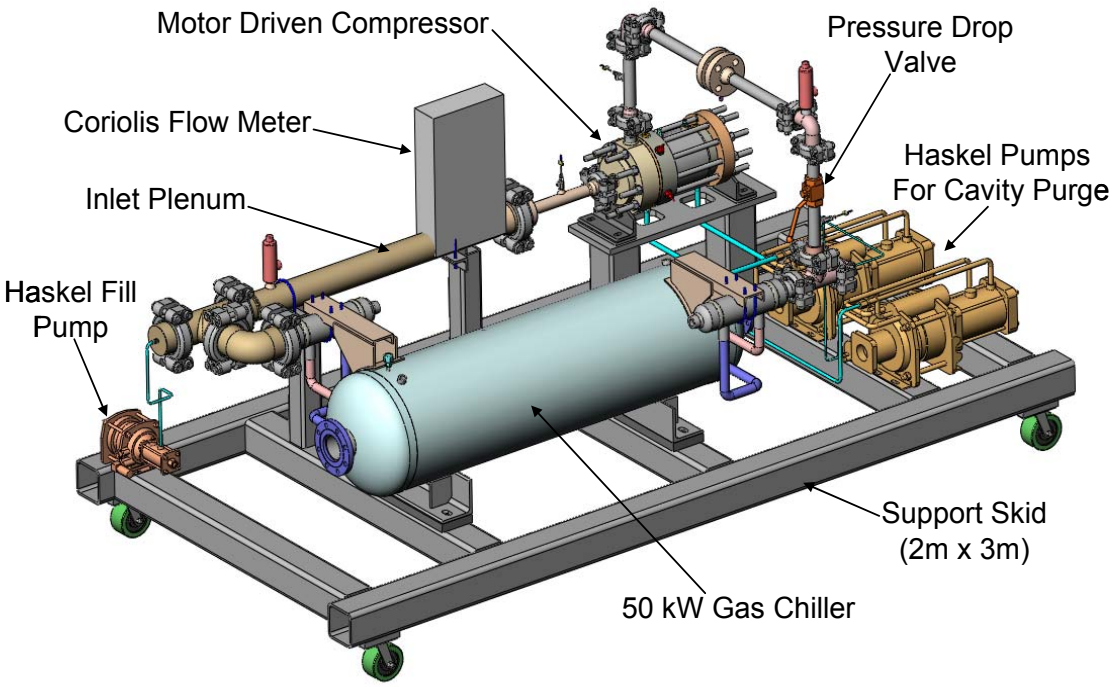

Figure 3-1: Engineering drawing of S-CO_2 Compression loop test skid.

A schematic layout of the compression loop, including the water cooling loop, is provided in Figure 3-2. Estimates of the state points, based on thermodynamic cycle analysis that show the temperature, pressure, flow rate, and power level of the components, are also provided. The "compression" loop consists primarily of a motor-driven radial compressor (~50 kW), a valve-controlled pressure drop orifice (in place of the turbine), and a gas chiller (50 kW). Typical operation of this loop consists of compressor speeds up to 45,000 rpm with a pressure ratio of 1.4 and a mass flow rate of 2.5 kg/s.

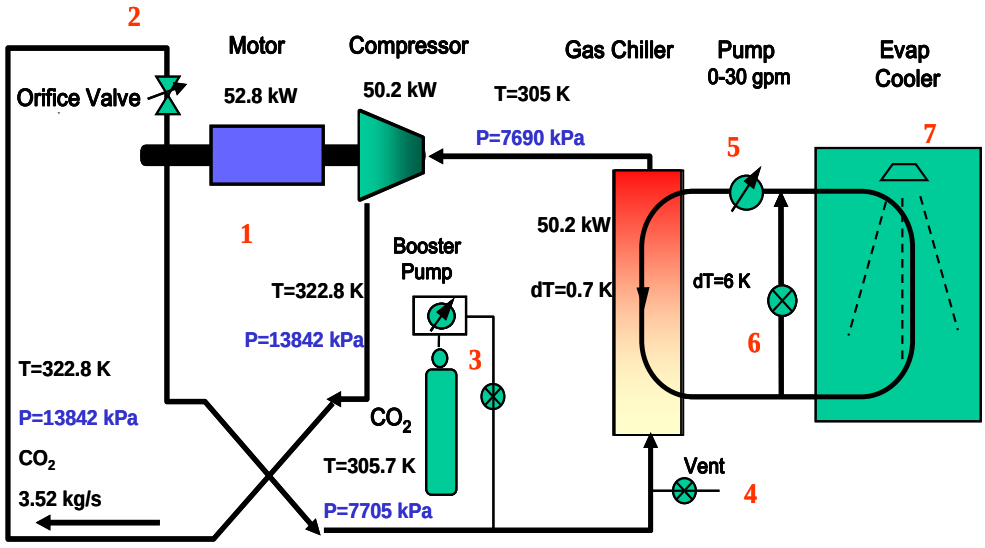

Figure 3-2: Schematic of supercritical compression loop using a 50 kWe motor driving a radial compressor at 75,000 rpm with a flow rate of 3.51 kg/s.

The turbomachinery is the key component in the S-CO_2 compression loop. It consists of a permanent magnet motor/alternator, the compressor, the diffuser vanes, the shroud, seals, bearings, and a water cooled housing. Figure 3-3 shows the details of the turbomachine and labels to identify the major components. The major function of the motor compressor is to spin the compressor wheel and thus provide pumping power to the CO_2. As much as 50 kW of pumping power can be supplied by the motor. At maximum conditions, the compressor wheel is designed to spin at 75,000 rpm and pump approximately 3.5 kg/s of supercritical CO_2 at a pressure ratio of 1.8. The compressor inlet pressure is just above the critical pressure and has a fluid density of approximately 57% the density of room temperature water.

The shaft is supported by gas foil journal and thrust bearings. These bearings are designed to allow the shaft to ride on a "pillow" of gas while they are spinning and provide a non-contacting no wear bearing. However, the rapid spinning of the permanent magnet rotor and gas foil bearings causes friction within the gas itself, known as windage. These windage losses are managed by pumping out the rotor cavity and keeping its pressure as low as possible (generally 150-300 psi) during operation. This windage also causes the bearings to heat up during operation. Excessive heating of the bearings has been the limiting factor for long-term operation of the device. Work is ongoing to improve the scavenging pump capability of the rotor cavity to minimize windage and heating, but also to provide localized cooling where needed.

Resistance Thermometry Devices (RTD's) which have an accuracy of ~0.2 K and thermocouples which have an accuracy of ~1 K are used to measure the fluid temperatures (water and CO_2). These devices are located in the CO_2 at the inlet and exit of every major component. Pressure transducers are also used to monitor the pressure at the inlet and outlet of every component. There is a Coriolis flow meter located at the inlet of the compressor that measures both mass flow rate and density of the CO_2.

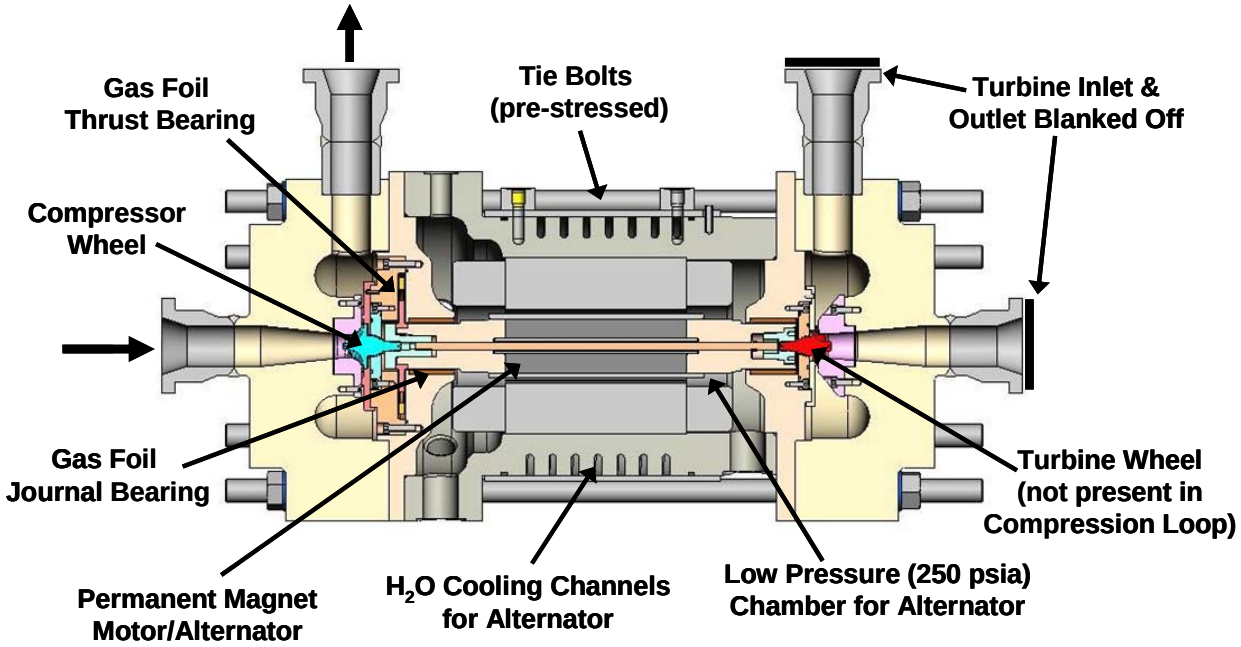

Figure 3-3: Schematic drawing of the motor-driven S- CO_2 compressor.

A photo of the as-built and assembled S-CO_2 compression loop located in SNL TA-3 is shown in Figure 3-4. The photo shows the grey motor control box on the right side of the image. The grey data acquisition and control box is located just above the motor controller. The data acquisition and control computer is located just off screen to the right.

Figure 3-4: Photo of the Sandia S-CO_2 compression loop as assembled at SNL.

4 CO_2 Compression Loop Operation with Condensation

The S-CO_2 compression loop described above has been modified to allow for more complete representation of a full condensing S-CO_2 Brayton cycle. This was accomplished by adding a second heat exchanger between the outlet of the compressor and the inlet to the CO_2 throttling valve, as shown in Figure 4-1. This heat exchanger is designed to add up to 50 kW of thermal energy to the CO_2. The secondary (shell) side of this heat exchanger is connected to a heated water loop.

The four locations at which the temperature and pressure state points are measured are illustrated Figure 4-1. These four points show the primary locations of temperature and pressure instrumentation in the primary CO_2 flow path. At each of these locations, both RTD and pressure transducers take data at a 1 Hz frequency. Also observe that just prior to station 1, a Coriolis flow meter is also used, which provides independent measurement of the fluid density at station 1. It measures the mass flow rate as well.

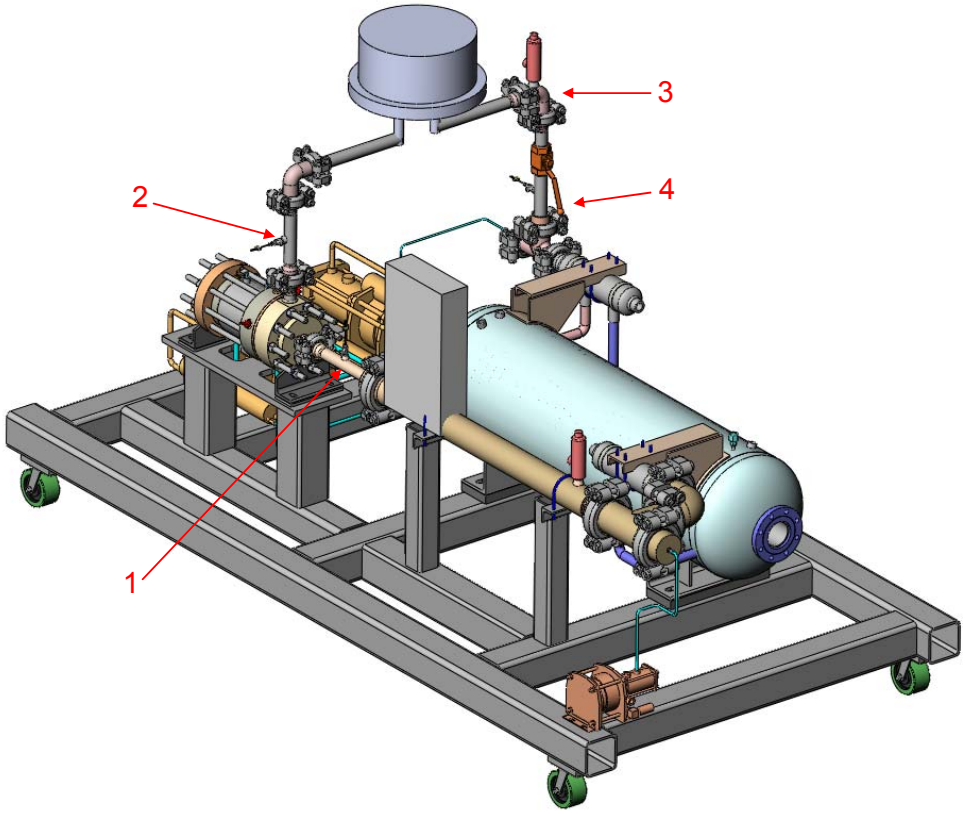

Figure 4-1: Engineering drawing of the S-CO_2 Compression loop with the addition of a head-addition heat exchanger. The red arrows point to the primary instrumentation locations.

A schematic of the flow path and state points in the modified compression loop is provided in Figure 4-2. The same state points shown in Figure 4-1 are again shown in Figure 4-2. Note that

state point 1 is shown in both the condenser exit and compressor inlet locations. This is because they are essentially identical state points, with only the flow meter and approximately 2-3 meters of piping between them. Typical values for mass flow, temperature, pressure, entropy, and enthalpy of the CO_2 at each state point are listed in Table 4-1. These values are also plotted on the temperature-entropy (T-S) diagram in Figure 4-3. The flow path is described below.

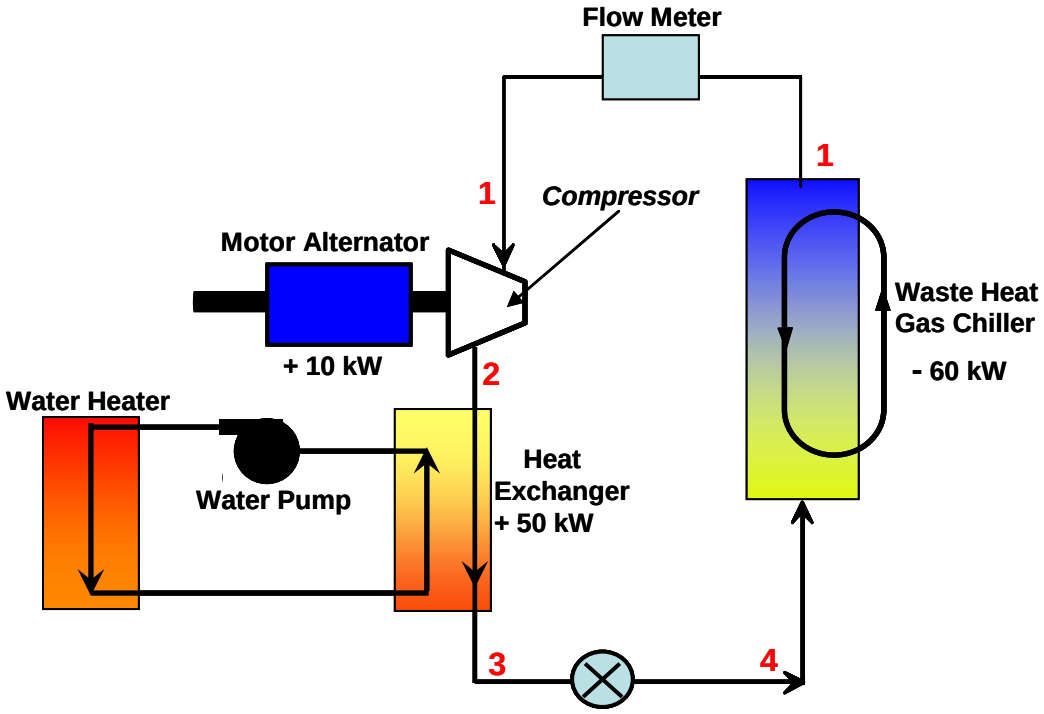

Figure 4-2: Schematic of the CO_2 compression loop in the condensing cycle configuration.

The motor driven compressor is used to pump CO_2 around the loop. While the motor is designed for operation up to 50 kW (at 75 krpm and 3.5 kg/s of flow), typical operation at 40-45 krpm require only 10 – 15 kW of motor power. In Figure 4-3, the compression is shown as being isentropic, increasing pressure from 7.1 MPa to 9 MPa. Once the CO_2 exits the compressor, the fluid enters the "heater" heat exchanger. This is a water-to-CO_2 heat exchanger that uses hot water from a secondary loop that flows through the shell side of this heat exchanger to provide up to 50 kW of thermal energy to the CO_2. In Figure 4-3, this is depicted as a constant pressure process, though some pressure drop (typically 1%) is expected in the actual system. The 50 kW of heat addition to the 1 kg/s flowing CO_2 results in an enthalpy rise of 50 kJ/kg, which increases entropy, pushingpushing the CO_2 towards the gas side of the saturation curvecurve. The water that circulates in a closed loop is heated with a Keltech Model CN543/480-D1-T200 water heater.

Table 4-1: Typical thermodynamic conditions of selected state points in the condensing CO_2 compression loop

State	Mass Flow [kg/s]	Temperature [K]	Pressure [MPa]	Entropy [kJ/kg-K]	Enthalpy [kJ/kg]
1	1	302	7.1	1.31	280
2	1	309	9	1.31	290
3	1	314	9	1.46	340
4	1	302	7.1	1.48	340

After leaving the heat exchanger, the CO_2 flows through a throttling valve. This valve takes the place of the turbine which is used in a full Brayton system. As the fluid flows through the partially-closed valve, its pressure drops to nearly the level of the compressor inlet. There is no heat addition or rejection across this valve, so this pressure change is assumed to be isenthalpic as shown in Figure 4-3. The partially-closed valve controls the CO_2 flow rate. In past experiments it has been possible to vary the flow from zero to 4 kg/s depending on the compressor shaft speed. For the test results presented here, the flow rate at 40-45 krpm is near 2 kg/s.

Upon exiting the throttling valve, the CO_2 continues to the "heat rejection" heat exchanger. The shell side of this heat exchanger contains water that flows in from an external evaporative cooler. The CO_2 flows through the tube side of the heat exchanger, and rejects heat to the colder water.

For the set of experiments described in this LDRD, this heat exchanger behaves as a condenser, and fully liquid CO_2 flow out of it into the Coriolis flow meter. The Coriolis flow meter measures the mass flow rate and density of the CO_2. The density measurementsmeasurements, as well as the noise levels in mass flow rate (two-phase flow through the meter produces a noisy signal) areare used to verify that single phase liquid is exiting the condenser and entering the compressor.

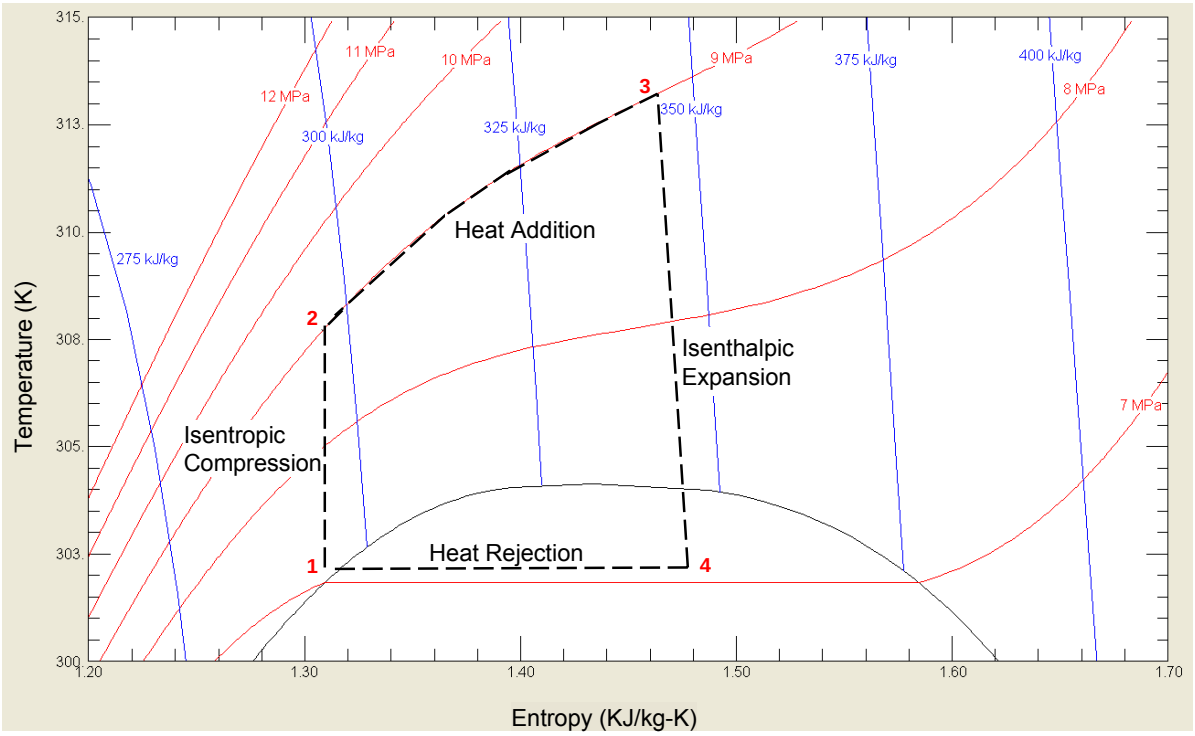

Figure 4-3: Predicted T-S diagram of the SNL CO_2 compression loop in the condensing configuration.

5 Testing

A condensing supercritical-CO_2 power cycle must have hardware that can accomplish three things on the cold side of the power cycle. First the compressor must be able to "pump" or compress liquid-like fluid densities;; second the pump/compressor must also be able to provide sufficient pressure rise when pumping liquids rather than gases;; and third the waste heat rejection exchanger (gas cooler) must be able to condense the CO_2 and thereby provide a continuous stream of liquid CO_2 when operated at the lower temperatures and pressures than the critical point.

Three types of experiments were performed to explore the behavior of the Sandia compression loop when operated as a condensing power system.

1. The first series of experiments were used to compress/pump liquid CO_2 using the S-CO_2 compressor.
2. The second series of experiments operated the compressor over a wide range of compressor inlet conditions that varied from pure vapor to pure liquid. These experiments also compressed two phase CO_2.
3. The third series of experiments made hardware modifications to the compression loop to heat the CO_2 after compression. The heater added sufficient enthalpy to the fluid (up to 50 kW) so that after expanding the CO_2 through the static valve, the fluid would either be a saturated gas or a two phase fluid well under the critical temperature and pressure.

Each of these three tests is summarized briefly below. More details are provided in the subsequent sections.

1. In a condensing supercritical-CO_2 power cycle (see Chapter 2), the compressor inlet properties consist of a fluid with liquid-like densities and with temperature and pressure below the critical point. For this reason, the first experiments of the condensing S-CO_2 LDRD project were arranged to evaluate the capability of using the supercritical CO_2 compressor to "pump" liquid-like CO_2 even though it was designed to operate near the critical point. The as designed compressor inlet temperature and pressure are 305.4 K and 7687 kPa with a density of 0.579 kg/liter. Because the loop is designed to operate at various compressor inlet temperature and pressures, the first series of tests could be performed with no modifications to the existing loop. The tests were performed by filling the loop to the appropriate fill mass and operating the gas cooler with sufficiently cold water so that the compressor inlet was a liquid. In these tests the CO_2 fluid density at the compressor inlet was 0.793 kg/liter. The liquid density of CO_2 at 850 psi (at standard bottle pressure and 85 F) is 0.615 kg/liter. Note that unlike water at room temperature, liquid CO_2, at temperatures and pressures near the critical point, is compressible.

2. Similarly, in a condensing cycle power loop the gas cooler must condense the single phase gaseous CO_2 and produce liquid phase CO_2. Normally in steam plants, condensers use gravity to separate the gas phase from the liquid phase. In this case because the gas phase and fluid phase are different in density by a factor of only 2-3, there was some question about the ability to separate the liquid from the vapor phase without re-designing the chiller. However the recent testing indicates that a tube and shell gas cooler, though not specifically designed as a condenser, was fully capable of providing

liquid CO_2 to the compressor for the subcritical conditions tested (see Section 6). Thus the goal of this series of tests was to observe the fluid density and phase of the gas chiller exit while its inlet was a single phase gas or a two phase mixture. Success was defined as achievement of single-phase liquid or two-phase conditions at the outlet of the orifice valve, with condensation occurring in the gas cooler with a pure single phase liquid fed to the inlet of the compressor.

3. The modified compression loop used the 50 kW heater to add enthalpy to the CO_2 fluid after compression. The experiments were performed with a compressor inlet temperature of 301-302K (83-85°F), and a pressure of 6900 - 7300 kPa. Because of the added enthalpy the measured results showed that the CO_2 entering the spiral tube and shell gas cooler was saturated vapor but the exiting fluid was saturated liquid CO_2. This verifies the ability of the gas cooler to condense the CO_2 at these conditions and the ability of the compressor wheel to pump the liquid CO_2 simultaneously. These test results were performed with a relatively small amount of sub-cooling below the critical point so the density difference between the liquid and the vapor is small (about a factor of 2). Presumably, depending on cooler design and degree of sub-cooling below the critical point it will no longer be possible to condense the CO_2. To date this has not been observed.

Though not detailed here, a fourth series of experiments was run at the SNL recuperated split-flow Brayton loop during which electric power was produced, while the main compressor and re-compressor operated in the two-phase region. In these tests, the compressor inlet conditions had a vapor quality of 89% at 297K (76°F). Future testing will explore the compressor inlet conditions that are closer to the liquid side of the saturation curve. Still, these tests reveal that the Brayton loop design, can operate with fractional liquid phase fluids, with a compressor that can compress the two phase fluid and condense the single phase CO_2 to a two phase mixture in the PCHE heat exchanger. This data has not yet been fully analyzed but provides further evidence that the condensing cycle is feasible using the existing turbomachinery.

Overall, the combination of tests show that the supercritical compressor can “pump” liquid like CO_2, that a even a tube and shell gas chiller heat exchanger, when fed two-phase CO_2, can produce liquid CO_2 which can be compressed by the main compressor when sufficient cooling is provided, that the main compressor is capable of compressing liquid, vapor, and two-phase CO_2, and that a simple heated recuperated Brayton cycle can produce net electric power while the compressor inlet is in the two phase regime. In total at this stage, these tests provide strong evidence that condensing S-CO_2 power cycles are indeed possible and the hoped for improvement in efficiency can therefore likely be achieved. More testing of this type is warranted and can be performed on the “modified” S-CO_2 compression cycle research loop, and on the simple heated recuperated Brayton cycle.

5.1 *Test results from the as-fabricated compression loop for liquid like compressor inlet conditions*

This first experiment uses the as fabricated ("unheated") Sandia compression loop to show that it is possible for the main compressor to effectively "pump" liquid CO_2 even though the compressor wheel was designed to operate near the critical point and not on the liquid side of the saturation curve. The T-S diagram corresponding to this test is illustrated in Figure 5-1. The test started the cycle with a high density liquid at the compressor inlet (1), compressing along a line of virtually constant entropy (1→2), then forcing the fluid through a flow restriction to cause a nearly isenthalpic pressure drop onto the saturation curve (2→3), before cooling in the chiller back to a subcritical liquid (3→1). As evidenced in Figure 3.1, the compression and pressure drop segments of this proposed scheme are almost vertical in orientation, providing only a slim or no margin for crossing into the two-phase regime at point 3. This explains the need to add a heater as detailed in Section 6.3.

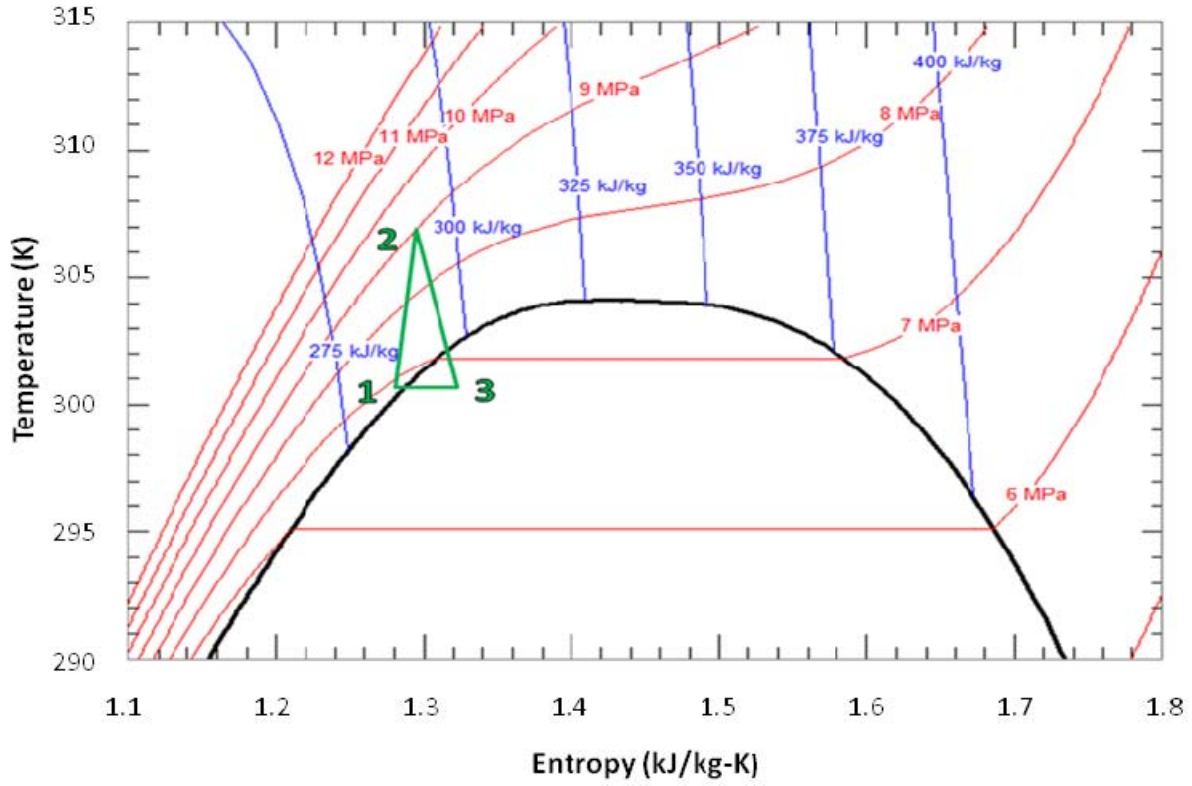

Figure 5-1: The CO_2 T-S diagram is shown for the compressor acting on liquid CO_2. The compressor inlet is shown at station 1, the compressor outlet at station 2, and state-points after expansion at station 3. These state-points are sketched in green.

Testing began with an experiment on 7/1/2010 (filename CBC_100701_12051205.csv).). The high density liquid desired at the compressor inlet for this series of tests was a departure from nominal operating conditions, which are normally just above the critical point. During the test, compressor speed was changed from 35,000 to 45,000 rpm in increments of 5 krpm, and at each speed the pressure drop valve was varied from a maximum of 45% open to a minimum of 30% in increments of 5%.

The experimental data for the 45 krpm segment of the test is shown in Figure 5-2. For the test results presented here, the coriolis meter was used to establish the state point at the compressor inlet by using temperature along with measured density, rather than pressure, to evaluate entropy using the tool Refprop. Due to discontinuities in calculated fluid properties near the saturation curve, this proved to be a far more stable method than using the temperature and pressure. At the compressor outlet, temperature and pressure were used to calculate entropy, since this point was sufficiently distant from the boundary of the saturation curve. At the restriction outlet, no additional instrumentation exists besides pressure and temperature sensors. Entropy at this point (station 3, purple x's) was instead estimated based on an isenthalpic assumption from the compression outlet, and on measured temperature. The red dots show the compressor inlet, the green triangles show the compressor outlet conditions at station 2. Because the valve was being closed in increments, there are four major lines at constant pressure corresponding to these valve settings. The purple x's show the state-point at station 3 downstream from the valve. The state-points correspond very nicely to the expected results illustrated in Figure 5-2, and thus effectively demonstrate the ability of the compressor wheel to work well with liquid CO_2.

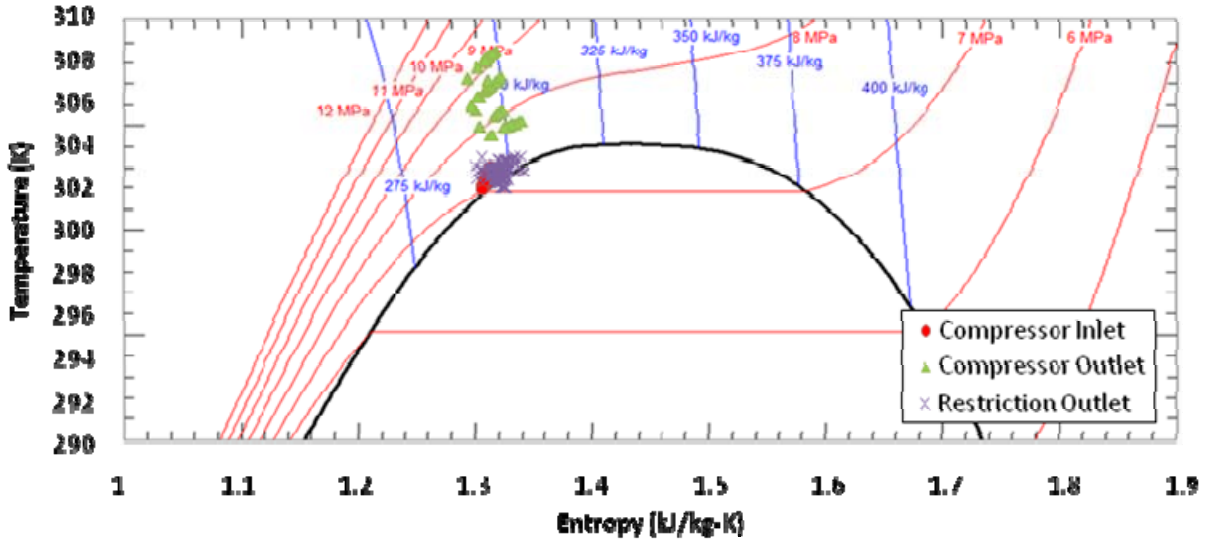

Figure 5-2: The CO_2 T-S diagram for the main compressor acting on liquid CO_2. The data is shown with experimental data based on measured compressor inlet density and temperature and assuming isenthalpic expansion for through the valve.

Despite the lack of condensing, these early tests provided valuable turbomachinery operating experience in the single-phase liquid CO_2 regime, which itself is an important verification of the feasibility of a condensing cycle.

Additional data from this series of tests was analyzed in order to generate compressor maps for compression in the liquid phase. Again, compressor speed was increased from 35,000 to 45,000 rpm in increments of 5 krpm, and at each speed the pressure drop valve was varied from a maximum of 45% open to a minimum of 30% in increments of 5%. The data generated in this experiment was used to plot the equivalent or 'corrected' ideal specific enthalpy rise as a function of corrected CO_2 mass flow rate, and is shown in Figure 5-3. The applied correction

factors transform conditions from each particular test point to dynamically similar conditions at a given reference temperature and pressure near the critical point, for ease of comparison.

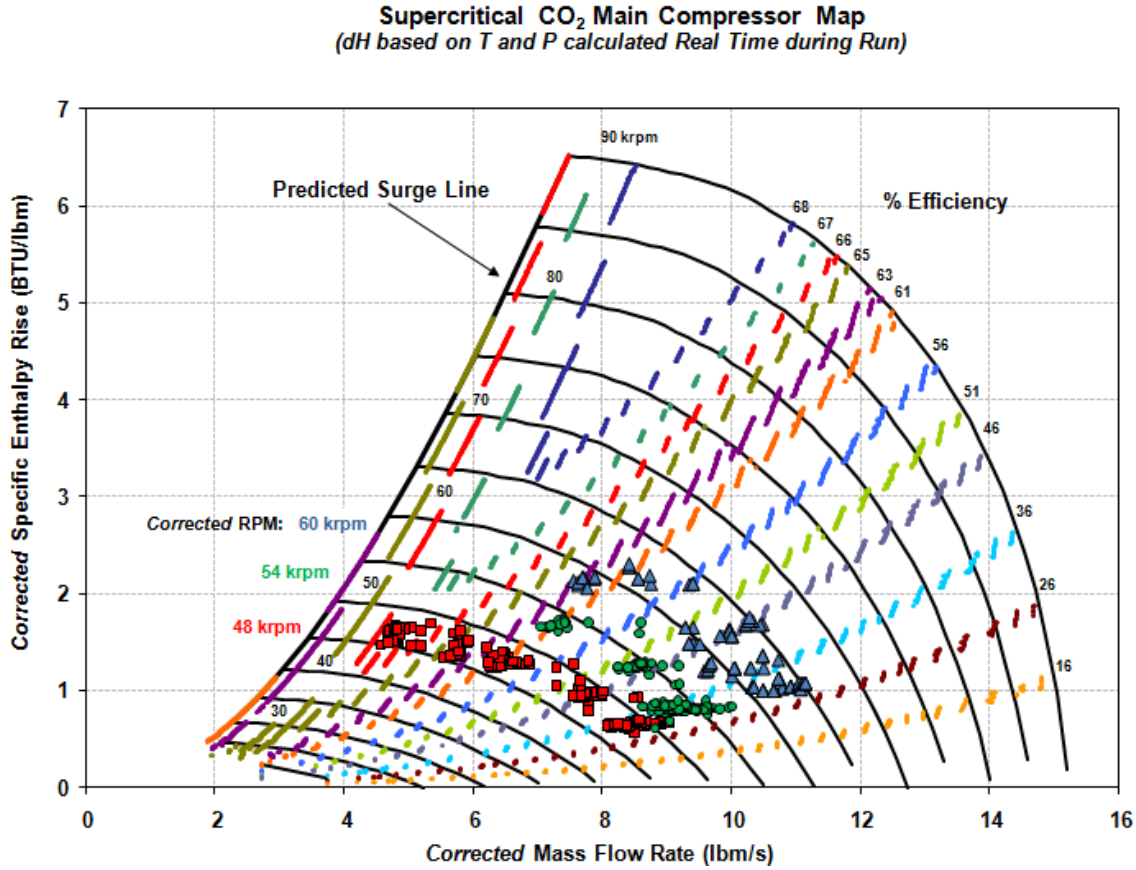

Figure 5-3: The compressor map is shown for compression of liquid CO_2 at 35, 40, and 45krpm.

The liquid-phase compressor tests proved that all components of the turbo-alternator-compressor could run smoothly up to 45 krpm, even though the unit was originally developed to study operation only at supercritical conditions. This work resulted in the recent publication *Supercritical-CO_2 Compression Loop Operation at Off-Nominal Conditions* (Radel et al 2010), which also examined operation with single-phase gas and two-phase conditions.

Though not specifically shown here, many experiments over the past few years, were performed with pure gaseous CO_2 at the compressor inlet. Generally these experiments show the compressor wheel operates well, the mass flow is stable, and that for vapor CO_2 the compressor pressure ratio is less than that seen in for liquid CO_2. This is expected because in essence the compressor produces a pressure ratio that is proportional to $\frac{1}{2}\rho v^2$ where ρ is the density and v is the tip velocity of the compressor wheel. Thus because liquid-like fluids have higher density they will also produce greater pressure ratios for a higher density fluid than for a lower density fluid.

5.2 *Compressor Wheel Operation for Liquid, Vapor and Two-Phase CO_2: The CO_2 Equation of State*

Previous testing has shown that the S-CO_2 main compressor can operate at off-design conditions including on the vapor and liquid sides of the saturation curve. Another series of tests is described here that shows that the S-CO_2 main compressor can also effectively compress two-phase CO_2 liquid-gas mixtures. Originally these tests were performed to investigate whether the critical point of CO_2 could be independently verified using the Sandia compression loop and instrumentation. If possible, this would help to establish a methodology for future efforts to determine the critical point of custom supercritical-CO_2/gas mixtures of interest to the condensing cycle, for which little data exists in literature.

Though these tests were performed originally to support the determination of the critical point for gas mixtures, they also show that the S- CO_2 main compressor wheel can effectively operate with a two-phase liquid-gas mixture of CO_2 as well. The ability of the S-CO_2 compressor to operate over such a wide range of conditions was attributed to two factors: the first is because the main compressor is a radial (centrifugal) compressor, rather than an axial compressor. Radial compressors are known to operate better over a range of fluid densities. The other reason is the small density ratio between the liquid CO_2 and vapor CO_2, at room temperature, (a factor of 3:1 for CO_2 compared to a 1000:1 for water). The results of these equation-of-state experiments are presented here because the ability of the compressor to pump two-phase CO_2.

The experiments began by qualitatively examining regions near the known critical pressure (1072 psi, 7.39 MPa). By taking temperature and density data along constant pressure lines near the critical point, the resultant curves provide an approximate metric for determining whether the fluid has reached the supercritical state. This uses the fact that, below the critical pressure, the CO_2 should exhibit a region (when it enters the saturation curve) where its curve adheres to a flat pressure/temperature relationship as density varies. At pressures above the critical pressure, the curves should pass over the dome without ever displaying this flat behavior.

The experimental procedure was as follows. The loop was first filled with dense liquid CO_2 at a designated pressure. PID control on the waste heat rejection loop was used to incrementally raise temperature. As the temperature increased it also causes the pressure to increase on both the liquid and vapor sides of the saturation curve. The loop was manually vented through a valve to release CO_2 gas, dropping inventory to keep the loop at constant pressure while the temperature continued to rise. Simultaneously, the compressor was run at 25 krpm to keep the loop inventory well-mixed. Test data taken at 1060 psi (7.31MPa) is shown below in Figure 5-4, just below the known critical pressure of 1072 psi (7.39 MPa).

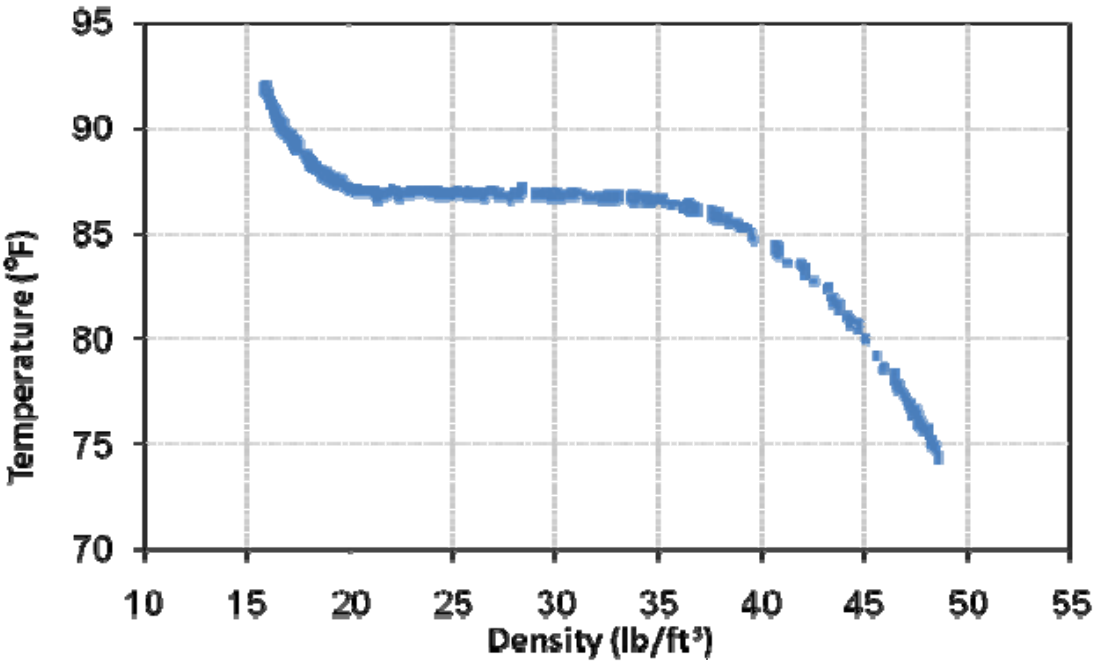

Figure 5-4: Experimental temperature and density data at a constant pressure of 1060 psi.

Data was filtered in post-processing to eliminate points more than 1 psi away from the designated pressure. A notable feature of the curve in Figure 5-4 is the flat region between the high density liquid and low density gas tails. This is clear evidence that two-phase conditions are possible at 1060 psi, and therefore that it is below the critical point.

Similar data was taken at other pressures to form a family of curves bounding the known critical point at 1000, 1060, 1080, and 1100 psi are shown in Figure 5-5. An initial observation of these curves is that they follow the constant pressure traces estimated by Refprop fairly closely, proving that the coriolis meter can be depended on for accurate measurements of density and mass flow through a range of two-phase flow regimes. Separately this experience also established that the compressor, seals, gas foil bearings, and other turbomachinery components can comfortably operate with two-phase conditions at the compressor inlet. While these curves help to show a transition from pressures below to those above the critical pressure, it's unlikely that this method of visual comparison can be depended upon to locate the critical point with precision better than ±20 psi. Additionally, this method would be far more difficult to attempt if the critical point was not known beforehand.

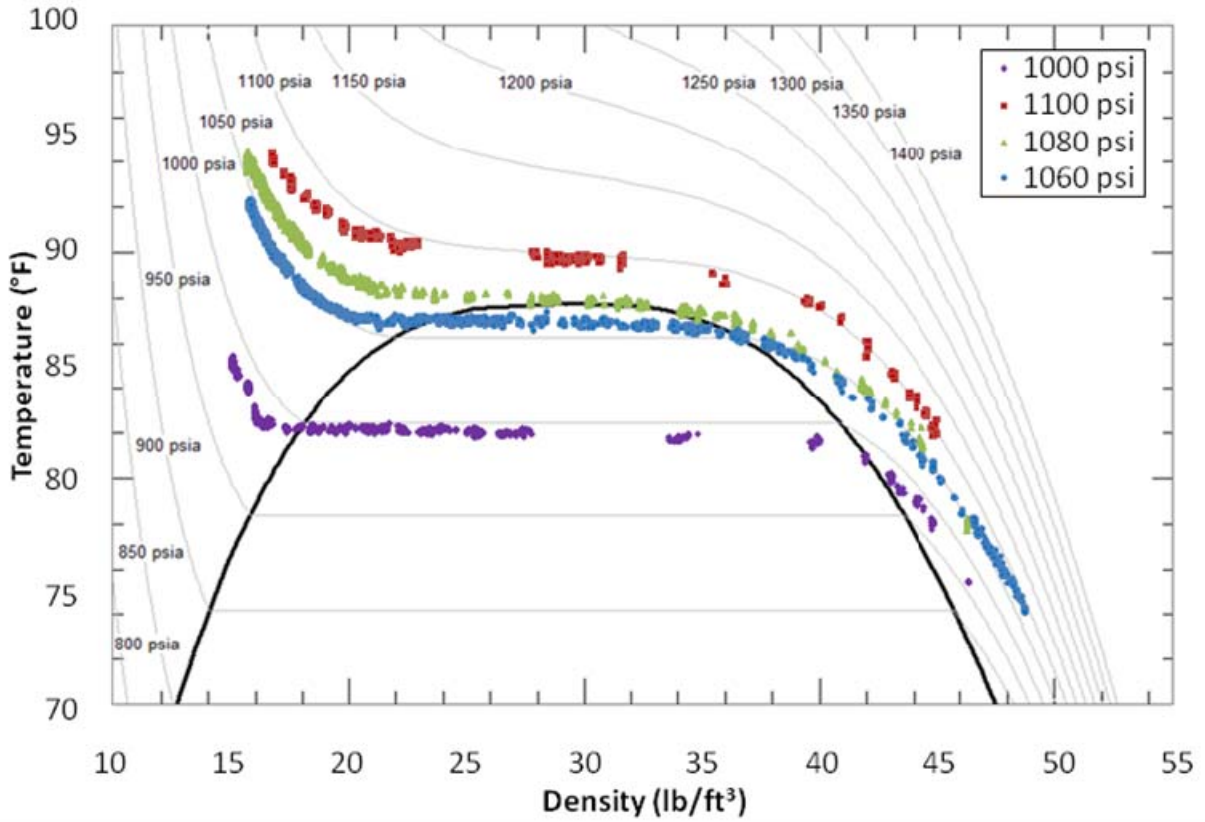

Figure 5-5: A comparison of constant pressure T-D curves at various pressures near the critical point.

5.3 *Condensing Experiments using the modified Compression Test Loop*

Once the SNL compression loop was modified to include the 50 kW heater, a series of experiments was performed to evaluate the feasibility of operating the compression loop as a condensing cycle. The goal of these experiments was to operate the compressor with a liquid CO_2 at the inlet, then heat the CO_2 about three degrees by adding the 50 kW and then expand the CO_2 through the variable nozzle to lower the pressure and either provide saturated vapor to the gas cooler or provide a two-phase mixture of CO_2 to the cooler. The cooler would then remove the excess heat from the compressor and heater to provide liquid to the compressor. Note that near the critical point, the heat capacity of the CO_2 is very large so at the test conditions of 1.4 kg/s flow (3.4 lb/s) the 50 kW was only able to heat the CO_2 about 3 K.

Figure 5-6 shows a representative two minute excursion during one of these experiments. The three graphs in this figure (A, B & C) show the measured time dependent pressure, temperature, mass flow, density and shaft speed. During this experiment, the compressor shaft speed was increased to 40,000 rpm and was held there for approximately two minutes. The pressure and temperature were held nearly constant during this experiment, although a slight increase in both was observed. In later experiments, a PID controller was employed to keep state points for the CO_2 fluid from drifting as in this test run. The CO_2 fluid at the compressor inlet was held at 85°F (303 K) and 1020 psia (7 MPa), with a flow rate of 3.4 lbm/s (1.5 kg/s). The compressor

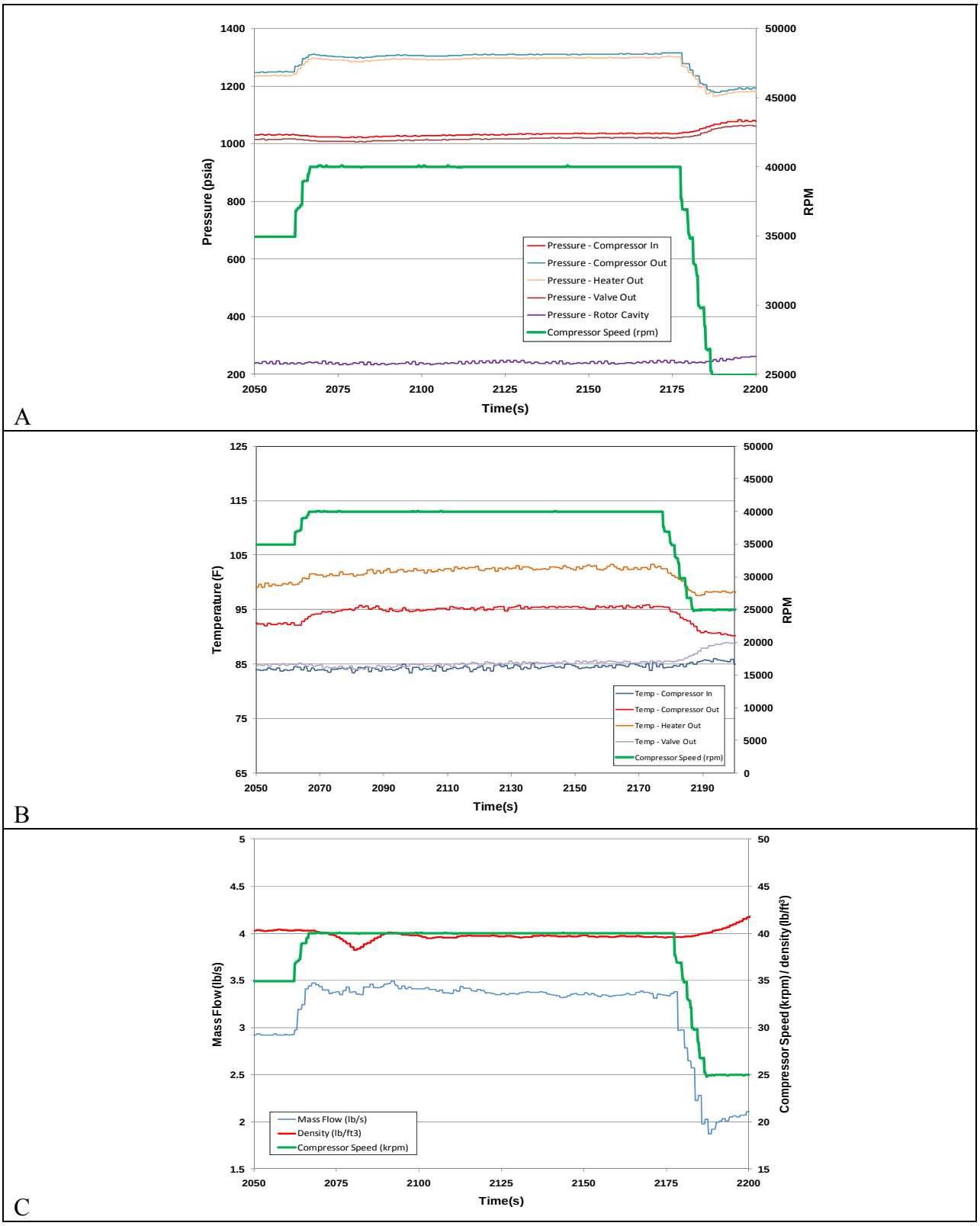

Figure 5-6: Pressure, temperature, mass flow, density, and compressor speed during operation of the SNL S-CO_2 compression loop

outlet pressure was 1300 psia (9 MPa), giving a pressure ratio of 1.27. Data was captured at a 1 Hz frequency and 30 seconds of data shown in Figure 5-6 have been plotted on the second T-S diagram in Figure 5-7 and Figure 5-8.

Thirty seconds of this data for the experiment described above are plotted on the second T-S diagram in Figure 6-7 (B). To populate these plots, the temperatures were taken directly from measured RTD data. The pressure was measured using the Honeywell FP2000 pressure transducers. A Micromotion coriolis flow meter was used to measure the compressor inlet density. The entropy is calculated using the NIST Refprop database. (Lemmon, 2007). The compressor inlet entropy is calculated using measured temperature and density values. The compressor outlet and heater outlet entropies are calculated using measured temperature and pressure values. This method is also used to calculate the entropy at the valve outlet in case (a). Note that this is possible because these state points are well outside the saturation curve. In cases (B) and (C), the entropy results from using temperature-pressure method are also shown for the valve outlet state point. However, because the fluid is in the two-phase zone, and the density is not known, Refprop provides only the vapor entropy. Tthese values are known to be incorrect because they do not conserve enthalpy for the isentropic expansion process that occurs in the valve. Since the values are inside the saturation curve the fluid is two-phase with some fraction of the fluid being a saturated liquid and the remaining a saturated vapor dome. If we had a density meter would be required at this location we could use density and pressure to directly calculate the entropy values, as is done at the compressor inlet. However, no such density meter exists in this experiment.

Instead, isenthalpic expansion is assumed in the valve. As seen in Figure 6-7 (A), this is a valid, though not perfect, approximation to make. Thus, the entropy information at the Valve Out – Corrected positions in Figure 6-7 (B) and (C) was obtained by using measured temperatures and by conserving enthalpy from the heater outlet position. Note that this correction was not required in Figure 5-7 (A) because the valve outlet position is well outside the vapor saturation curve.

The three curves in Figure 5-7 show that as the sub-cooling (below the critical point) is increased the T-S points illustrating the paths of compression, heating, expansion and condensation are clearly shown by the measured state-points as measured at the exit of the compressor, heater, valve, and gas cooler. As the gas is cooled below the critical point it is also necessary to increase the fill mass of the system to assure that the exit conditions from the gas cooler are liquid and not a two-phase mixture. Thus some form of inventory control is required to increase or decrease the loop fill mass must be provided in any system that wishes to use the "condensing" S-CO_2 power cycle.

Figure 5-7 (B) and (C) clearly show that condensation of the CO_2 working fluid is occurring between that valve outlet and compressor inlet state points. As shown in Figure 3-2, a tube-in-shell heat exchanger is located in this position. While this heat exchanger was not designed to operate as a condenser, it does an effective job as one. This may be due to the relatively small difference in density between gaseous and liquid CO_2. In full-scale power plants, this behavior may allow heat rejection equipment to be designed for "standard" S-CO_2 Brayton operation, but still be used for condensing operation. This provides an increased

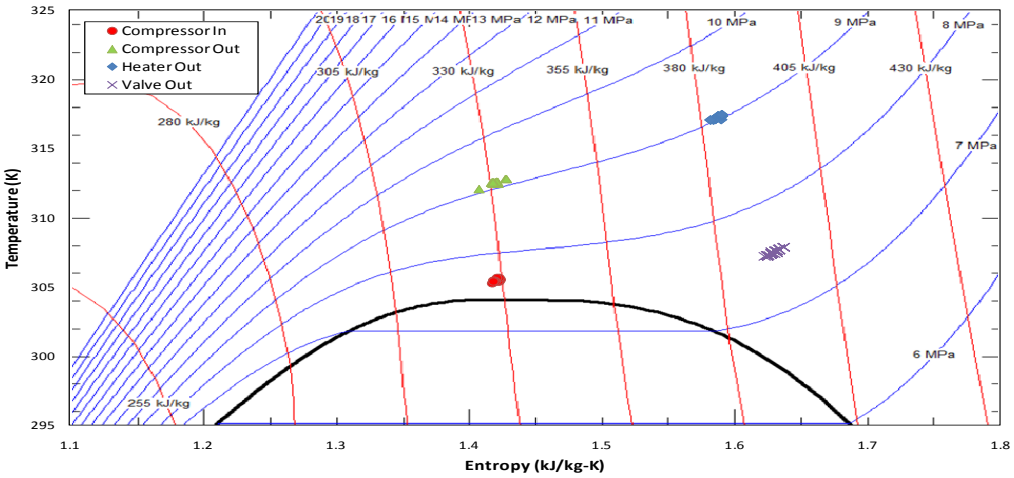

A

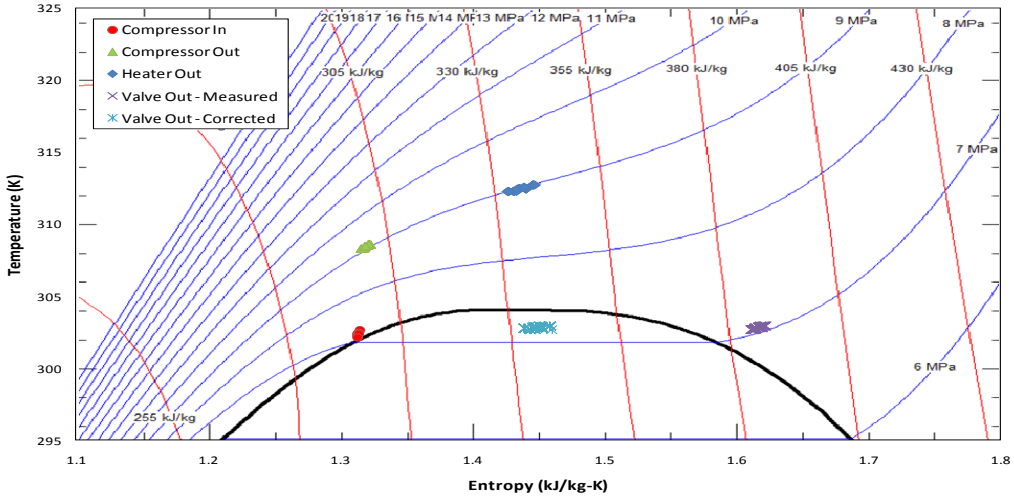

B

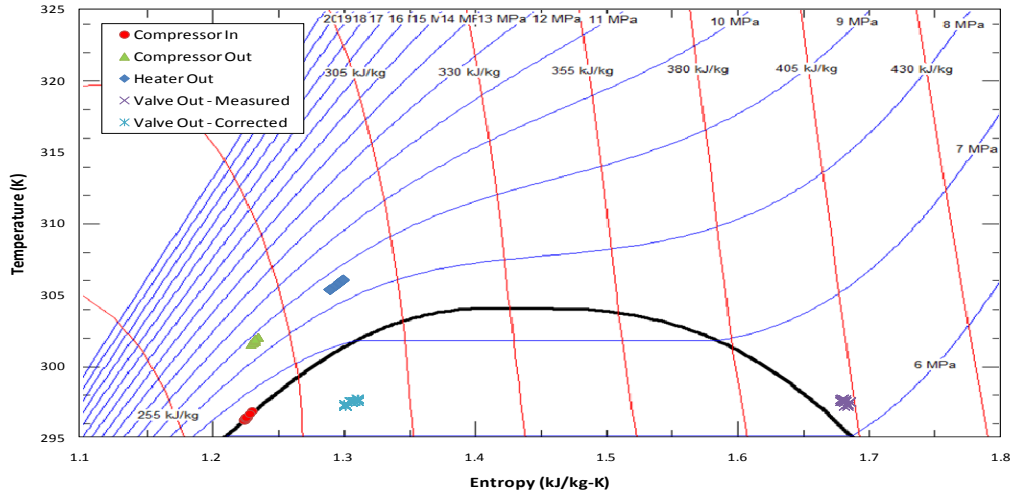

C

Figure 5-7: T-S diagram of S-CO_2 compression loop with: (A) supercritical CO_2 at compressor inlet. (B) T-S diagram of S-CO_2 compression loop with liquid CO_2 (303 K) at compressor inlet. (C) liquid CO_2 (296 K) at compressor inlet.

efficiency with no additional hardware requirements and allows the system to take advantage of colder heat rejection temperature when available

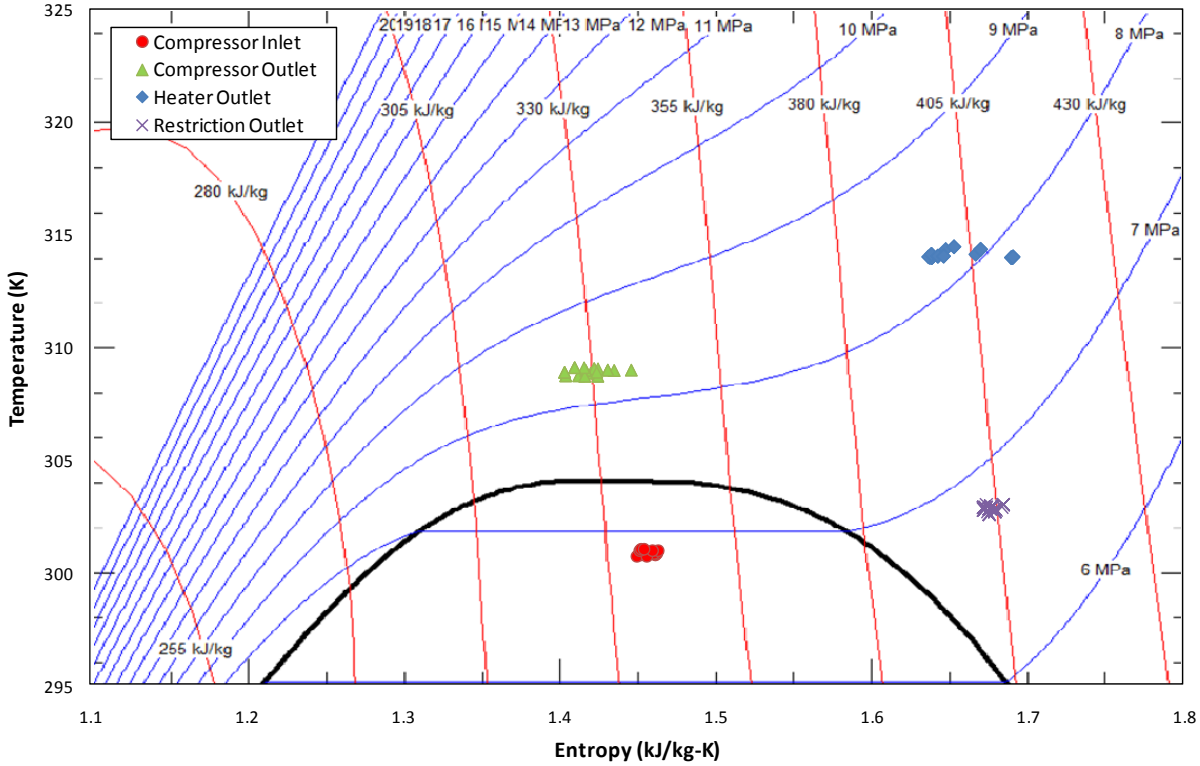

Figure 5-8: T-S diagram of S-CO_2 compression loop with two-phase liquid CO_2 (296 K) at compressor inlet.

6 Summary and Conclusions

Though the S-CO_2 Brayton cycle has shown promise as a power conversion system for advanced high temperature reactors, conventional wisdom was that the lower outlet temperature of LWRs (~600K) would rule out the use of Brayton cycle technology. The CO_2 "condensing" cycle described in this work breaks this barrier by establishing that, according to computational models, conversion efficiency of up to 39% (up from 34%) is possible by lowering the compressor inlet temperature to 295K, pumping liquid CO_2 into the compressor, and forcing condensation of CO_2 vapor to take place in the cold leg. Also because of the greater pressure ratio required in the compressor and turbine, it is possible to add multiple stages of reheat which also increase the efficiency. These characteristics describe a cycle (condensing re-compression cycle with multiple stages of reheat) which is, on the cold side, more reminiscent of the Rankine cycle used at steam plants. It was also found that another 2% of efficiency (41% total) can be converted by raising the LWR outlet temperature by 30°C, though effects on the reactor system itself were not examined.

Furthermore, the cost savings associated with the much smaller CO_2 power conversion system is another factor which favors the "condensing" cycle over the larger power conversion cycle used by steam plants. Large-scale supercritical CO_2 systems are estimated to be about 1/10th the size of a comparable steam plant, and therefore have the potential to dramatically reduce capital costs. The reduced scale can be attributed to the high density of CO_2 near the critical point, and to the relatively small ratio of liquid-to-gas CO_2 density during condensing (3:1), in comparison to 1000:1 for water.

In parallel, an experimental program demonstrated the feasibility of operating closed Brayton cycle turbomachinery and other loop components in the range of conditions required for the condensing cycle. Tests were carried out to run the compressor using a high density liquid CO_2 at inlet, which yielded compressor maps at several rotation speeds showing high efficiency and large compression ratios. Another series of tests involved operating the compressor at low speed (25krpm) while tracing constant pressure lines of CO_2, from a liquid, through the two-phase zone, and into the gas phase. The stable operation of the compressor, all other components, and consistent readings of the instrumentation during these scenarios instilled confidence that the loop was capable of operating and generating meaningful data at all necessary points.

Finally, a 50kW heater was added to the loop in order to simulate a heated Brayton cycle. Again the compressor was operated with single-phase liquid inlet conditions, the fluid was heated, and then passed through a restriction and into the two-phase saturation region ("dome"). Here, the gas chiller acted as a condenser, providing a saturated liquid to the compressor. This demonstrated that the spiral chiller could be used as-designed for the purpose of condensing, requiring no separator or hardware modifications. These results imply flexibility in operating conditions that would allow a full-scale plant to be designed for "standard" S-CO_2 Brayton operation, but used for condensing when cooler temperatures are available.

This study has illustrated the benefits that can be realized by combining LWRs (and other low to moderate temperature heat sources) with the supercritical CO_2 Brayton power conversion cycle, through the use of a reduced waste heat rejection temperature to cause condensing. Future efforts will investigate this effect further by introducing supercritical fluid mixtures which alter the critical temperature, allowing another degree of freedom. From the work described here and that being performed in concurrent studies, the supercritical CO_2 cycle is emerging as a system which the picture of stable operation over a diversity of conditions and applications, in contrast to early concerns that the system would be hostage to a narrow, unstable band.

7 References

Angelino G., "Perspectives for the Liquid Phase Compression Gas Turbine", Journal of Engineering for Power, Trans. ASME, Vol. 89, No. 2, pp. 229-237, April, (1967).

Angelino G., "Carbon Dioxide Condensation Cycles for Power Production", ASME Paper No. 68-GT-23, (1968).

Angelino G., "Real Gas Effects in Carbon Dioxide Cycles", ASME Paper No. 69-GT-103, (1969).

Barber-Nichols Inc. Contractor Report to Sandia National Laboratories, Robert Fuller, Ken Nichols, Bill Batton, Jeff Noall, "Small Scale Power Systems and Turbo-Machinery Assessment Using Super Critical Carbon Dioxide Working Fluid", October 4, 2006.

Barber Nichols Incorporated, www.barber-nichols.com, Arvada, CO, USA 2010

Buongiorno J. and MacDonald P., "Supercritical Water Reactor (SCWR): Progress Report for the FY-03 Generation-IV R&D Activities for the Development of the SCWR in the U.S", INEEL/EXT-03-01210, September 30, 2003.

Dostal, V., Driscoll, M., Hejzlar, P., "A Supercritical Carbon Dioxide Cycle for Next Generation Nuclear Reactors", MIT-ANP-TR-100, (2004).

Heatric, a Meggit Group, www.heatric.com, Dorset, UK, 2010.

Lemmon, E.W., Huber, H.L., McLinden, M.O, REFPROP – A Computational Tool for Reference Fluid Thermodynamic and Transport Properties, NIST Standard Reference Database 23, Version 8.0, (2007).

Pratt and Whitney Rocketdyne, Canoga Park, Ca, Contractor Report to Sandia National Laboratories, "Design of a small Scale Test Loop to Demonstrated Power Generation with Supercritical CO_2", October 31, 2006.

Radel, R.F., Conboy, T.M., Wright, S.A., "Supercritical-CO_2 Compression Loop Operation at Off-Nominal Conditions" *(to be published)*, Proceedings of the ANS Winter Meeting, Las Vegas, NV, (2010).

Sandia National Labs, "Working Fluids and Their Effect on Geothermal Turbines" SNL sub proposal to ORNL CEEB-180, February 12, 2009.

Wright, S., Radel, R., Vernon, M., Rochau, G., and Pickard, P., "Operation and Analysis of a Supercritical CO_2 Brayton Cycle", SAND2010-0171, (September 2010).

Wright, S., Radel, R., Vernon, M., Schriner, H., and Pickard, P., "Generation IV Brayton Cycle Test Loop Design and Split-Flow Compressor Test Loop Construction Description", Generation IV Energy Conversion Level 2 Milestone Report, Work Package G-SN08VH0101 (September 15, 2008).

Vogta, B., Fischera K., Starflinger J., Laurienb E., Schulenberg T., "Concept of a pressurized water reactor cooled with supercritical water in the primary loop", *Nuclear Engineering and Design,* 20 May 2010.

Wright S., "Optimum Power Cycle Efficiency using "Tunable" Supercritical Gas Mixtures for Supercritical Brayton Cycles", Sandia Technical Advance No: SD 11594, January 7, 2010.

8 Distribution

EXTERNAL Electronic Distribution

Agronne National Laboratory
James Sienicki, ANL/NE, sienicki@anl.gov
Anton Moisseytsev, ANL/NE, amoissey@anl.gov
Dae Cho, ANL/NE, cho@anl.gov
Richard Vilim, ANL/NE, rvilim@anl.gov
Robert Hill, ANL/NE, bobhill@anl.gov

Barber Nichols Inc
Bob Fuller, bfuller@barber-nichols.com
Bill Batten, bbatton@barber-nichols.com
Ken Nichols, knichols@barber-nichols.com

Bechtel Power Corporation
Kenneth J. Kimball, kimbal@kapl.gov
Justin Zachary, jzachary@bechtel.com

Bettis Atomic Power Laboratory
Dave Vargo, david.vargo@unnpp.gov
Rich Siergiej, Richard.siergiej@unnpp.gov

Department of Energy
Tom O'Connor, DOE/NE-33, tom.o'connor@hq.doe.gov
Rick Kendall, DOE/NE-74, rick.kendall@nuclear.energy.gov
Matt Hutmaker, DOE/NE-32, matthew.hutmaker@nuclear.energy.gov
Dick Black, DOE/NE-3, Richard.Black@Nuclear.Energy.gov
B.P. Singh, DOE/NE-51, bhupinder.singh@nuclear.energy.gov
John Kelly, DOE/NE-7, JohnE.Kelly@nuclear.energy.gov

Idaho National Laboratory
Chang Oh, chang.oh@inl.gov
Lee O. Nelson, Lee.Nelson@inl.gov
Mike Patterson, mw.patterson@inl.gov
James Werner, james.werner@inl.gov

Institute of Nuclear Energy Research, INER
Yea-Kuang Chan, ykchan@iner.gov.tw

Distribution Cont.

Knolls Atomic Power Laboratory
Ken Kimball, KAPL/103, kennith.kimball@unnpp.gov
Rudy Cuervo,KAPL/103, Rodolfo.cuervo@unnpp.gov
Joseph Nehrbauer,KAPL/103, Joseph.ehrhauer@unnpp.gov
Joe McDonnell/ KAPL/103, Josheph.McDonnel@unnpp.gov

MIT Department of Nuclear Science and Engineering
Michael Driscol, mickeyd@mit.edu
Ron Ballinger, hvymet@mit.edu

NASA Glenn Research Center
Chris DellaCorte, christoperher.dellacorte@nasa.gov
Lee Mason, Lee.s.mason@nasa.gov

Natural Resources Canada
Kourosh E. Zanganeh, kzangane@nrcan.gc.ca

Northrop Grumman Shipbuilding (Newport News, Va. Shipyard)
Rick Connolly, rick.connolly@ngc.com
Michael Rapp, mp.rapp@ngc.com
Michael J. Reilley, Michael.Reilley@ngc.com
John M. Spain, John.Spain@ngc.com

Oak Ridge National Laboratory
Sherrell Greene, greenesr@ornl.gov
Daniel Ingersoll, ingersolldt@ornl.gov
Joanna McFarlane, mcfalanej@ornl.gov
Lou Qualls, quallsal@ornl.gov

Thar Energy, LLC
Marc Portnoff, marc.portnoff@tharprocess.com

Tokyo Institute of Technology
Yasuyoshi Kato, kato@nr.titech.ac.jp

University of Wisconsin Madison
Mark H. Anderson, manderson@engr.wisc.edu

Distribution Cont.

Internal Distribution

George A. Backus MS0370 (1465) gabacku@sandia.gov
E. Tito Bonano MS0736 (6220) ejbonan@sandia.gov
Ben B. Cipiti MS0747 (6223) bbcipit@sandia.gov
Thomas M. Conboy MS1136 (6222) tmconbo@sandia.gov
Laura A. Connolly MS0736 (6220) laconno@sandia.gov
Rich Diver MS1127 (6337) rbdiver@sandia.gov
Darryn Fleming MS1136 (6222) ddflemi@sandia.gov
Patrick J. Griffin MS1146 (6221) pjgriff@sandia.gov
Gary Harms MS1146 (1384) gaharms@sandia.gov
Ronald Lipinski MS0747 (6774) rjlipin@sandia.gov
S. Andrew Orrell MS0771 (6200) sorrel@sandia.gov
Gary Rochau MS1136 (6221) gerocha@sandia.gov
Larry R. Shipers MS1007 (6531) lrshipe@sandia.gov
Nate Siegel MS1127 (6337) nsiege@sandia.gov
Ellen Stechel MS0734 (6339) ebstech@sandia.gov
Marjorie L. Tatro MS0721 (6100) mltatro@sandia.gov
Milton Vernon MS1146 (6221) meverno@sandia.gov
Marianne Walck MS0701 (6700) mcwalck@sandia.gov
Steven A Wright MS1146 (6221) sawrigh@sandia.gov
D. L. Chavez, LDRD Office MS0359 (1911) dchavez@sandia.gov
Technical Library MS0899 (9536) librpts@sandia.gov

Sandia National Laboratories